ISSN 1590-8844
Vol. 14 No 01
2013

International Journal of Mechanics and Control

Editor: Andrea Manuello Bertetto

LIBRERIA EDITRICE UNIVERSITARIA
LEVROTTO & BELLA
TORINO

Official Torino Italy Court Registration
n.5390, 5th May 2000

Deposito presso il Tribunale di Torino
numero 5390 del 5 maggio 2000
Direttore responsabile:
Andrea Manuello Bertetto

International Journal of Mechanics and Control

The Journal is addressed to scientists and engineers who work in the fields of mechanics (mechanics, machines, systems, control, structures). It is edited in Turin (Northern Italy) by Levrotto&Bella Co., with an international board of editors. It will have not advertising.

Turin has a great and long tradition in mechanics and automation of mechanical systems. The journal would will to satisfy the needs of young research workers of having their work published on a qualified paper in a short time, and of the public need to read the results of researches as fast as possible.

Interested parties will be University Departments, Private or Public Research Centres, Innovative Industries.

Aims and scope

The *International Journal of Mechanics and Control* publishes as rapidly as possible manuscripts of high standards. It aims at providing a fast means of exchange of ideas among workers in Mechanics, at offering an effective method of bringing new results quickly to the public and at establishing an informal vehicle for the discussion of ideas that may still in the formative stages.

Language: English

International Journal of Mechanics and Control will publish both scientific and applied contributions. The scope of the journal includes theoretical and computational methods, their applications and experimental procedures used to validate the theoretical foundations. The research reported in the journal will address the issues of new formulations, solution, algorithms, computational efficiency, analytical and computational kinematics synthesis, system dynamics, structures, flexibility effects, control, optimisation, real-time simulation, reliability and durability. Fields such as vehicle dynamics, aerospace technology, robotics and mechatronics, machine dynamics, crashworthiness, biomechanics, computer graphics, or system identification are also covered by the journal.

Please address contributions to

Prof. Guido Belforte
Prof. Andrea Manuello Bertetto
PhD Eng. Elvio Bonisoli

Dept. of Mechanics
Technical University - Politecnico di Torino
C.so Duca degli Abruzzi, 24.
10129 - Torino - Italy - E.C.

www.jomac.it
e_mail: jomac@polito.it

Subscription information

Subscription order must be sent to
the publisher:

Libreria Editrice Universitaria
Levrotto&Bella
2/E via Pigafetta – 10129 Torino – Italy

www.levrotto-bella.net
e_mail: info@levrotto-bella.net
tel. +39.011.5097367
+39.011.5083690
fax +39.011.504025

ISSN 1590-8844
International Journal of Mechanics and Control, Vol. 14, No. 01, 2013

Preface for the special issue of the JoMaC dedicated to the 21st edition of the Workshop on Robotics in Alpe-Adria-Danube Region, RAAD 2012

This special Journal issue is obtained as a result of a selection and second review process from the best papers that were accepted for RAAD 2012 Workshop.

The 21st edition RAAD 2012 of the RAAD Workshop gathered researchers of the robotics community mainly from countries of the Alpe-Adria-Danube region, in a collegial and creative environment. Coherently with its tradition, RAAD 2012 covered all the major areas of robotics research and applications, from fundamental to applied research.

The workshop made possible a forum for significant scientific and technical discussions pointing at the most recent developments in the field of robotics, renewed professional contacts and strengthened the participants' technical expertise. Social and cultural events with the wonderful Napoli historical sites were also planned to facilitate exchanges of ideas, opinions and experience among the attendees.

The mission of RAAD Workshops is to promote research and development in the field Robotics within the geographical European area of Alpe-Adria-Danube countries by facilitating contacts and exchanges among institutions and researchers.

The RAAD Workshop is a well-established forum in the field of European Robotics. After the start up of 1992 in Portorož (Slovenia), it has been held every year in different European countries: 1993 Krems (Austria), 1994 Bled (Slovenia), 1995 Pörtschach (Austria), 1996 Budapest (Hungary), 1997 Cassino (Italy), 1998 Bratislava (Slovakia), 1999 Munich (Germany), 2000 Maribor (Slovenia), 2001 Vienna (Austria), 2002 Balatonfüred (Hungary), 2003 Cassino (Italy), 2004 Brno (Czech Republic), 2005 Bucharest (Romania), 2006 Balatonfüred (Hungary), 2007 Ljubljana (Slovenia), 2008 Ancona (Italy), 2009 Brasov (Romania) , 2010 Budapest (Hungary), 2011 Brno (Czech Republick). In the year 2012 the event was host it in Napoli.

The 21st edition of the RAAD workshop was organized by the DiME, Department of Mechanics and Energetics of the University of Naples 'Federico II' in partnership with LARM, Laboratory of Robotics and Mechatronics of the University of Cassino and South Latium in September 11 to 13, 2012. The event was also sponsored by IFToMM, the International Federation for the Promotion of Mechanism and Machine Science, Engineering Union of Napoli Provence, and ASME Italy Section.

After the review process 51 papers by authors representing 9 different countries were accepted for publication in the proceedings volume of RAAD2012 together with the keynote lecture by prof Marco Ceccarelli, Italy and prof Gregory Chirikjian, USA. The RAAD 2012 collected the most recent research results in Robotics. The Technical Program Committee has defined an outstanding program in quality and diversity. The presented topics reflect trends in analysis, modelling, design and integration of robot systems in various fields of activity and applications, such as history and manufacturing, services and health care, surgery and human rehabilitation, education and collaborative projects, space investigation, tele-operation and control, grasping and manipulation, guidance vision and automated visual inspection.

We would like to express our sincere gratitude to the members of the scientific committee for the support and help both in Workshop organization and paper selection for this journal special issue:

Guido Belforte, Polytechnic of Turin, Italy
Theodor Borangiu, University of Bucharest, Romania
Marco Ceccarelli, Technical University of Cassino and South Latium, Italy
Karol Dobrovodsky, Academy of Sciences, Slovakia
Stefan Havlik, Academy of Sciences, Slovakia
Nick Andrei Ivanescu, Technical University of Bucharest, Romania
Roman Kamnik, University of Ljubljana, Slovenia
Zdeněk Kolíbal, University of Brno, Czech Republic
Gernot Kronreif, Integrated Microsystems Austria
Doina Pîslă, Technical University of Cluj□Napoca, Romania
Andreja Rojko, University of Maribor, Slovenia
Cesare Rossi, University of Napoli, Italy
Imre J. Rudas, Óbuda University, Budapest, Hungary
Leon Zlajpah, Jožef Stefan Institute, Slovenia

We believe that RAAD 2012, hosted in Napoli, represented an important moment for the activity of our RAAD Organization in sustaining innovative R&D projects of the robotics science and technology, not only in Europe.

ISSN 1590-8844
International Journal of Mechanics and Control, Vol. 14, No. 01, 2013

This special Journal issue has been obtained as a result of a selection and second review process, but all the papers that were accepted for RAAD 2012 were of good quality with interesting contents and it has been hard to decide for the selection. Perhaps some papers did not received due attention for this special issue from reviewers but we hope that the authors have decided for a submission to a journal yet.

We thank the authors who have contributed excellent papers on different subjects, covering many fields of Robotics. We are grateful to the reviewers for the time and effort they spent evaluating the papers.

We would like to thank the publisher and Editorial staff of this journal and particularly the Chief Editor prof Manuello Bertetto for accepting and helping the publication of this special issue within the established tradition of the RAAD Workshops.

We believe that this journal special issue on RAAD 2012 Workshop can be an interesting reference for the European activity in the fields of Robotics as wells as a source of inspirations for future works and developments.

Napoli and Cassino, March 2013


The Guest editors: Cesare Rossi and Marco Ceccarelli, Co-Chairs of RAAD 2012

ISSN 1590-8844
International Journal of Mechanics and Control, Vol. 14, No. 01, 2013

DESIGN AND EVALUATION OF DRIVE TRAIN CONCEPTS FOR A 3-DOF ROBOTIC STRUCTURE

Tim Detert* Stefan Kurtenbach* Burkhard Corves*

* RWTH Aachen University: Department of Mechanism Theory and Dynamics of Machines, Germany

ABSTRACT

This paper introduces a systematic approach to the drive train design for 3-DOF robotic arms integrated in a new kind of parallel-kinematic manipulator. After a short introduction into the state of the art, the methodology and main considerations are presented. They are applied to gain a set of principle solutions for possible drive-trains of each link. The design process is carried out developing nine different concepts from this solution set. Subsequently, relevant evaluation criteria are introduced, explained and their quantitative values are determined. Finally, the evaluation of the concepts is accomplished for given requirements and a weak point analysis is performed for two concepts.

Keywords: evaluation, robotic arm, manipulator, parallel kinematic, drive train design

1 INTRODUCTION

The department of mechanism theory and dynamics of machines (IGM) of the RWTH Aachen developed and designed the novel flexible and versatile handling concept PARAGRIP, based on a reconfigurable architecture with a modular layout [1, 2]. The robot system is able to handle objects with six degrees of freedom (DOF) by forming a parallel kinematic structure including several robotic arms and the object itself. One robotic arm possesses six DOF, with only the regional structure driven by three servomotors. This reduces the number of drives of the complete handling system to nine motors to handle the object with three translational and three rotational DOF (see Figure 1). In comparison using cooperating standard robots 18 motors in three robots are needed for similar tasks.

After a brief overview over the state of the art, the motor position and orientation are discussed. A set of principle solutions for the actuation of the links of the robotic arm is developed by variation of the motor position, motor orientation and drive train design.

These principle solutions are combined resulting in 9 different concepts, feasible for the parallel manipulators. Considering the future goal of a manipulator with good dynamic properties and high accuracy, quantitative evaluation criteria are developed and the according attributes are calculated for every concept. Based on these criteria, the 9 concepts are evaluated and additionally their general properties, advantages and disadvantages are discussed. Finally, a weak point analysis depicts the properties of 2 selected concepts graphically.

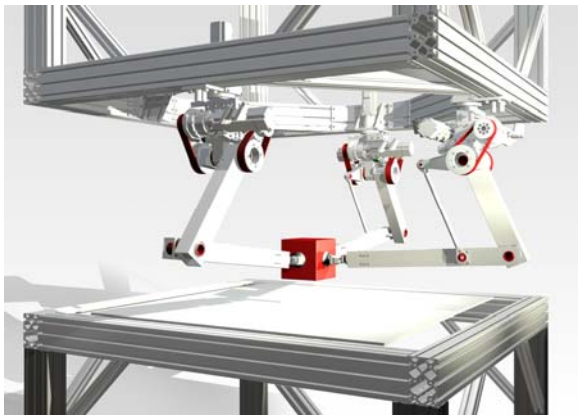

Figure 1 Final PARAGRIP prototype after including the handling object.

Contact author: Tim Detert[1], Stefan Kurtenbach[2]

[1]detert@igm.rwth-aachen.de
[2]kurtenbach@igm.rwth-aachen.de

2 STATE OF THE ART

At present there is no systematic approach for the conceptual design of the drive train for a robotic arm in general. However, there are many works regarding the components of a drive train.
Roos [3] follows a discrete approach for the selection of gears, transmission ratio and motors from a given set of available options for a single motor drive train. Therefore the weight, size, peak power, torque and efficiency of the drivetrain are taken into account, while the backlash and accuracy are not considered, even though they might be highly relevant depending on the application in robotics.
The optimal transmission ratio and selection of the best motor where mainly investigated for serial structures: Van de Straete [4] developed a selection criterion, separating the motor characteristics from the load characteristics by normalisation of the motor torque, velocity and transmission ratio.
Choi [5] expands Van de Straete's criterion by a selection criterion for the power limit of the motor and a temperature based criterion for steady state operation.
Petterson [6, 7] developed an optimization algorithm for drive trains in serial structures, where the influence of the motors to each other is taken into account. While motor characteristics are calculated using continuous variables, different available gearboxes are calculated using discrete variables.
Only few novel drive train concepts appear in literature: Karbasi [8] introduced a new drive train concept where the robot-joints are driven by a central and flexible shaft. A gearbox for each joint converts the moment and direction of rotation as needed, while the position and speed of the joints can be controlled using a clutch. The single modules are relatively lightweight compared to a motor used for every joint.
In the BioRob Project [9] a device with wire rope drive trains was developed for research purpose. Alternative to very stiff and usually heavy drive trains, compliant drive trains offer some advantage because of a lightweight design and compliance in case of a collision. Adversely, low stiffness leads to high requirements regarding the measuring and control technology.

3 MOTOR POSITION AND ORIENTATION

The given kinematic arm-structure used for the manipulator has three revolute joints with one DOF each. Link 1, attached to the main axis of rotation (MAR), link 2 and link 3, connected by the joints A and B, need to be driven by the motors 1, 2 and 3 (Figure 2). To do so, different variations of the motor position and orientation are possible and will be investigated.

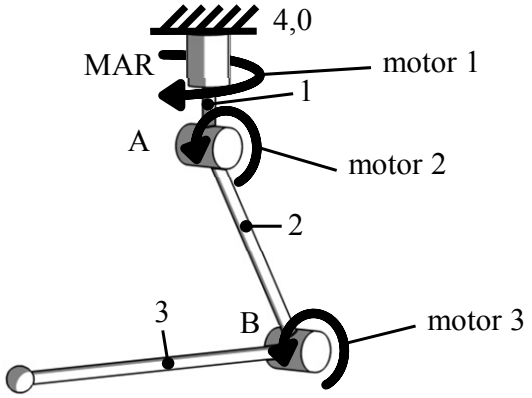

Figure 2 Driven joints and axes on the arm structure.

The moment of inertia (MOI) effective on the motors is decisive for the dynamic behaviour of the structure. While the MOI of the drive train and the motor itself are not altered by the motor position/orientation, the MOI effective on motor 1 is influenced by the arrangement (serial vs. parallel) and position/orientation of the motors 2 and 3. The MOI effective on motor 2 is influenced by the position and orientation of motor 3 if a serial arrangement is chosen. On the one hand, motors attached with their centre of mass close to the MAR or joint A have a small radius of inertia (ROI) in the moving arm structure, even more, attached to the base the MOI effective on the motors is zero. On the other hand attaching the motors close to the driven links reduces the length of the drive train and hence potentially increases the stiffness of the drive train and reduces its mass, backlash, package dimensions and complexity. Therefore different motor positions/ orientations on the base 4;0, link 1 and link 2 need to be investigated, aiming for a sufficient trade off. Positioning a motor on link 3 is not reasonable, as it would induce a MOI effective on motor 3, without benefits for the length of the drive train, compared to a motor positioned on link 2.
If a motor is attached to the driven link or to the link next to it, there is no complex relative motion that needs to be compensated by the drive train. For example link 2 rotates around joint A and hence the according motor 2 can be attached easily to link 1 or 2. Attaching it to the base would demand a complex drive train due to the two degrees of rotation of link 2 relative to the base. Additionally the orientation of the motor might complicate the design of the drive train depending on the position of the driving and the driven axis relative to each other.

4 PRINCIPLE SOLUTIONS

Different variations of the motor position, motor orientation and drive train design are possible and lead to a set of principle solutions, shown below. A more detailed description of the motor positioning and design of the drive train can be found in [10].The

principle solutions were selected from the large number of theoretically possible combinations by qualitative benchmarking of their feasibility.

The first set of principle solutions introduces the actuation of link 2 with motor 2 attached to link 1. In Figure 3a a bevel gear is used for the drive train, with the motor axis parallel to the MAR. Figure 3b is analogue to the first one, in this case the motor is positioned parallel to the axis A and the torque is transferred by a spur gear drive. Figure 3c presents the servomotor in the same position. In this case a form-fit traction belt transfers the torque. Figure 3d shows the torque transmission via a two bar linkage driving link 2. Figure 3e suggests a mounting of the servomotor directly at the axis A without an additional drive train.

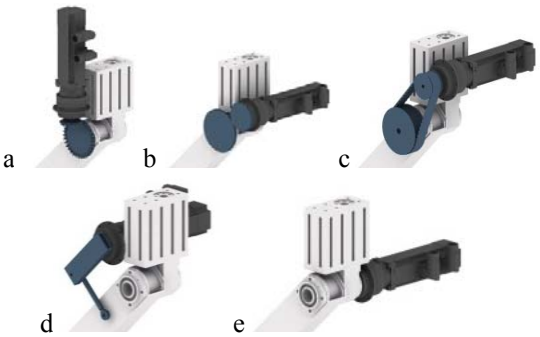

Figure 3 (a-e) Motor 2 positioned at link 1.

In Figure 4 principle solutions with the motor mounted at the base are shown. The general advantage is the fixed position of the drive, not inducing a moment of inertia (MOI) effective to any of the motors. However, transmitting the torque to the driven links needs several transmission elements, again increasing the MOI.

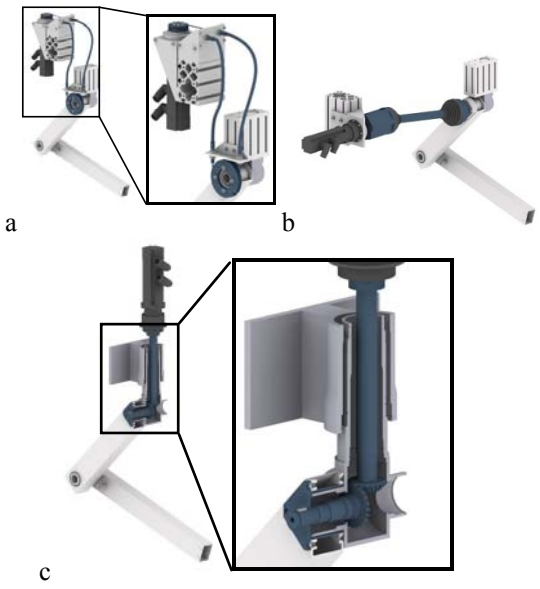

Figure 4 (a-c) Motor 1 positioned at the base.

In Figure 4a the transmission of a traction force by Bowden-cables is shown. Here, every direction of rotation requires a separate cable for the transmission. In Figure 4b two homokinetic joints with a connecting shaft are shown. The joint mounted at the motor is able to move in axial direction to compensate the rotation of the two bar linkage around the MAR. The bending angle of the homokinetic joints mounted at link 1 limits the workspace of the two bar linkage to a ±45° rotation around the MAR. The homokinetic joint mounted at the motor features an axial stroke of 75 mm, which enables the required axial motion of the shaft. Furthermore this solution induces a relatively high MOI because of the comparably large radius of inertia. The last Figure 4c emphasizes the utilization of a hollow shaft and a bevel gear to transmit the torque. Advantageous is the small cross-section. The rotation angles are not limited but the production effort is very high.

Figure 5 represents the arrangement of motor and transmission elements driving link 3 with the motor mounted to link 2. In Figure 5a a shaft transmits the torque via a bevel gear across the joint B. Figure 5b shows the motor flange mounted at the joint B. This requires no additional transmission elements for the drive train, but results in a high radius of inertia.

Figure 5 (a-b) Motor 3 positioned at link 2.

In the group of principle solutions shown in Figure 6 the torque is transmitted to link 3 from a motor mounted to link 1, with the advantage of reduced MOI compared to the solutions shown in Figure 5. The motor is mounted close to the MAR, which ensures a short radius of inertia. Figure 6a shows a flange mounted motor and a traction belt transmitting the torque to link 3. The second mechanism (Figure 6b) combines the two bar linkage and a form fit belt drive, resulting in a very small radius of inertia relative to the MAR and hence a low MOI effective on motor 1. In the resulting parallelogram, the alignment of the links (singularities) needs to be avoided. This does not limit the workspace significantly. According to the proposed handling concept, only the arm-workspace in front of the arms is needed, forming the common workspace of the system. Figure 6c differs from the second one through the non-collinearity of two-bar linkage joint,

which causes a variable transmission ratio between motor 3 and link 3, depending on the position of the two-bar linkage.

Figure 6 (a-c) Combination of motor 3 at link 1 and transmission between A and B.

5 CONCEPTS

For driving the links 2 and 3 the principle solutions can be combined arbitrarily but reasonable, which originates a diversified set of solutions. The solution set was decreased systematically by qualitative and quantitative benchmarking and direct comparison of the possible concepts during the design process, taking the feasibility into account. 9 different concepts resulting from the principle solutions were design to detail and are described in the following.

The motor 1 is flange mounted to the base in every concept. The advantage of this is the short drive train and stiff bearing for the overall rotation. Mostly similar or identical concepts for the drive of link 2 and link 3 are combined to obtain solutions with uniform properties over the whole workspace.

The direct actuation of link 1 with a the servomotor mounted directly at the axis A without an additional drive train (Figure 3e) offers many possibilities for the choice of a principle solution for the drive train of link 2. The direct actuation is implemented in the concepts A to D (Figure 7 and Figure 8). Therefor these concepts allow a good comparison of the principle solutions used for the actuation of the second link, applied to a detailed design.

The torque transmission to link 1 via a two bar linkage (Figure 3d) is very challenging in the practical design. The dimensions of the two additional links are mainly determined by the working range. This results in poor transmission behaviour and extreme transmission ratios close to the end positions. Therefor this principle solution was only used once in concept E as shown in Figure 9.

Concept F, shown in Figure 9 is similar to concept A (Figure 7), but additionally using a form-fit traction belt for the transmission of torque. This concept facilitates a comparison of solutions with a form-fit traction belt and direct actuation without an additional drive train, applied to a detailed design.

The huge advantage of the concepts G, H and I shown in Figure 10 and Figure 11 is the comparatively low MOI around the MAR. In comparison to all before introduced concepts, where the heavy servomotors in interplay with the radius of inertia cause a high MOI, these concepts propose the mounting of all servomotors at the base. Furthermore the link 2 solely is driven across a two bar linkage which forms a parallelogram with link 1 and 2. Certain machine elements transfer the generated torque to the respective input link.

In Concept A, shown left in Figure 7, link 1 is driven directly by the servomotor, there is no additional drive train. The second link is driven via a two bar linkage. The two motors are arranged parallel to each other on one side of the MAR to reduce the size ratio. By this arrangement, the axis of motor 3 and link 1 are not collinear, and the two bar linkage, link 1 and link 2 do not form a parallelogram. Therefor the transmission ratio between motor 3 and link 2 is dependent on the position of the arm.

In Concept B, shown right in Figure 7, link 1 is driven directly by the servomotor and the second link is again driven via a two bar linkage. By arranging the two motors collinear, the two bar linkage, link 1 and link 2 do form a parallelogram, resulting in a constant transmission ratio between motor 3 and link 2.

Figure 7 Concepts A (left) and B for the actuation of the arm.

In Concept C, shown left in Figure 8, link 1 is again driven directly with motor 2 collinear to motor 3. Link 2 is driven via a form-fit traction belt. Using a form-fit traction belt does require a constant distance between the driving axle and driven axle or a spring-driven belt pulley in the return strand. As the return strand changes with the rotational direction, the driving axle has to be collinear to axis A and therefor an alternative arrangement of the motors is not possible in such a concept.

Concept D, shown right in Figure 8, is the most basic one, with both motors attached directly to the according links. This serial structure has considerably different properties compared to the parallel structures of the other concepts. Velocity and

acceleration of the two motors sum up at the end effector, allowing higher speeds at the end effector at a given motor speed. For the same reason, the necessary driving torque for motor 2 increases at a given end effector force.

Figure 8 Concepts C (left) and D for the actuation of the arm.

In concept E, shown left in Figure 9, both links are driven via a two bar linkage. The motors are arranged parallel to each other and close to the MAR to reduce the MOI. Similar to concept A the transmission ratios between motor 2 and link 1 and motor 3 and link 2 are dependent on the position of the arm. As mentioned above, this dependence is very disadvantageous at the end positions.
In concept F, shown right in Figure 9, link 1 is driven by a form fit traction belt while the second link is driven by a combination of a two bar linkage and a form fit belt drive. Similar to concept E, the arrangement of the motors results in a low MOI effective on motor 1.

Figure 9 Concepts E (left) and F for the actuation of the arm.

In concept G, shown left in Figure 10, Bowden cables are applied. The generated torque is transformed into a tractive force by a pulley, mounted on the shaft of the servomotor. Subsequently, Bowden cables, one for each traction direction of one input link, transmit this force to a further pulley which is mounted on the respective input link. The servomotor driving the MAR is directly flange mounted at link 1. This concept possesses a low MOI because the moving mass is reduced to a minimum. Disadvantageous is the comparatively low stiffness of the Bowden cables.

Figure 10 Concepts G (left) and I for the actuation of the arm.

Concept I, shown right in Figure 10, bases on the interlacing of two hollow and one solid shaft. The torque is transferred via a solid shaft respectively a belt drive plus hollow shaft across a bevel gear to the respective input link. This concepts builds very compact and is comparatively stiff. It possesses a high mass and costs, both founded in the high number of bearings, complex shafts and belt drives.
In concept H, shown in Figure 11, two constant velocity drive shafts are driving the respective links. The constant velocity joint next to the linkage possesses a bending angle of 54° which limits the rotation around the MAR to ±45°. The constant velocity joint next to the servomotor has a small bending angle of about 18° but enables a linear stroke of 75 mm. This stroke is required because of the rotation of the linkage close to the constant velocity joint. An advantage of this kind of joint is the transfer of angular speed with a transmission ratio of 1. Disadvantageous is the limited working range.

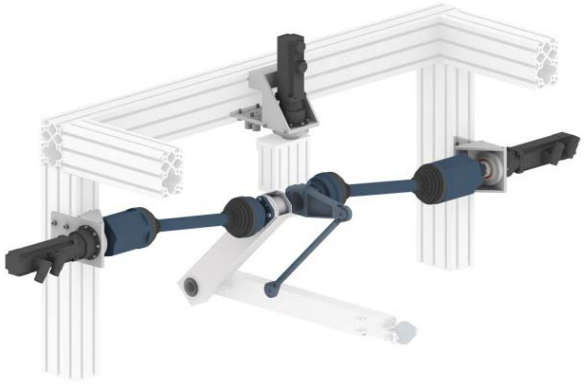

Figure 11 Concept H for the actuation of the arm.

6 EVALUATION CRITERIA AND CALCULATION OF THE ATTRIBUTES

As the properties of the 9 concepts differ strongly from each other, depending on the requirements of the manipulator, the best concept can be chosen using an appropriate evaluation in dependence on the VDI 2225 [11]. Therefore a set of quantitative evaluation criteria, which can be obtained with adequate effort, is needed. They represent the properties relevant for the fulfilment of the given task or requirements of the manipulator. In this chapter the nine criteria

- low compliance,
- low backlash,
- low moment of inertia,
- low mass,
- low size ratio,
- low static torque,
- high working range,
- low variability of transmission ratio and
- low costs

are evaluated and the calculation procedure for the according attributes is shown briefly.
As the criteria are of different relevance, weighting factors have to be determined. Their values are between 0 and 1 and the sum of the nine weighting factors is 1. The values of the criteria were determined using a preference matrix, were the importance of all the criteria is compared with each other in pairs of two. The resulting weighting factors are shown in Table I.

6.1 COMPLIANCE

The compliance of the structures influences the accuracy of the parallel manipulator due to distortion under loading conditions. It is described as the movement $\vec{\delta k}$ of the end effector due to a given static load $\vec{F}$:

$$\vec{\delta k} = C_{tot} \cdot \vec{F} \tag{1}$$

Where C_{tot} is the total compliance matrix. It incorporates the compliance of the links, the motors, the drivetrains and the kinematic properties of the structure, dependent on the position of the arm. It is calculated using the Jacobian matrix J_p and the compliance matrix C of the structure:

$$C_{tot} = J_p^{-1} \cdot C \cdot J_p^{-T} \tag{2}$$

$$C_{tot} = \begin{pmatrix} c_x & c_{xy} \\ c_{yx} & c_y \end{pmatrix} \tag{3}$$

c_x (c_y) describes the compliance in x (y) direction if a load is applied in x (y) direction. c_{xy} (c_{yx}) describes the cross-compliance in x (y) direction if a load is applied in y (x) direction. The bending and compression stiffness of the links and the torsional stiffness of the drive train and the motor are incorporated in C. It is a 2x2 matrix and describes the variation of the driving angle $\delta\vec{\varphi}$ at a given torque $\vec{T}$ effective on the driving axle:

$$\delta\vec{\varphi} = C \cdot \vec{T}. \tag{4}$$

C can be obtained relatively easy, using beam theory for the stiffness of the links and technical specifications of the drive train components and motors. The stiffness of the joints is not taken into account.
For the evaluation, the mean of the value of the total compliance matrix C_{tot} was calculated for 40000 positions in the central area of the work space.

6.2 BACKLASH

The rotatory backlash φ_{out} of the drive train as a whole is another factor influencing the accuracy of the parallel manipulator. Changes in direction or load lead to a break in the movement of the structure. Therefore, drive trains with very low backlash are needed. Many standard machine elements, e.g. bevel gear and the planetary gear of the servomotor, introduce backlash to a drive train. The backlash φ_{out} effective on the motor was calculated, taking the transmission ratio of the drive train into account:

$$\varphi_{out} = \frac{\varphi_{in}}{i} \tag{5}$$

In this equation i is the respective transmission ratio and φ_{in} is the respective backlash of the particular machine element. The linear clearance Δs, found in bearings connecting the links, can be approximately expressed as an equivalent rotatory backlash $\varphi_{out\ eq}$ by multiplication with the length l of the lever:

$$\varphi_{out\,eq} = \Delta s \cdot l. \tag{6}$$

For the evaluation, the overall backlash of the drive train is calculated as the sum of the backlashes of all individual machine elements.

6.3 MOMENT OF INERTIA

The MOI influences the dynamic behaviour of the robotic structure, a low MOI results in lower driving torques needed for acceleration and deceleration. The MOI effective on the different motors is dependent on the position of the arm structure and can be determined for each element of the drive train relative to its axis of rotation. The inertia of elements performing a translational movement can be expressed as an equivalent MOI J_{eq} by multiplication of the mass m with the length l of the lever:

$$J_{eq} = l^2 \cdot m. \tag{7}$$

The values were calculated by the CAD-System on base of the definition of the material and the volume of the elements.

For the evaluation the values where calculated for two different arm positions, both representative for the movement tasks of the given parallel kinematic structure.

6.4 MASS

The mass of the whole robotic structure including all elements of the drive train as well as the drives influences the flexibility, transport and reconfigurability of the parallel manipulator; therefor it should be rather low. Analogue to the MOI, the values of the mass are determined through the CAD-System and its sum is evaluated.

6.5 SIZE RATIO

The size ratio reflects the required space of a single robotic arm necessary to avoid the risk of a collision with other robotic arms while working in combination.
For the evaluation, the radius of a rotation around the MAR is calculated, using the point with the largest distance to the MAR. Again the CAD-Model is used for measuring the values.

6.6 STATIC TORQUE

The static torque is applied by the servomotors when there is no load connected to the end effector and the robotic arms are stopped. In this situation the motors have to procure the torque correlative to the weight of the robotic structure. A general force analysis is carried out using the equilibrium conditions. In this way the equivalent static torque for the motors 2 and 3 can be calculated.
For the evaluation the values where calculated for two different arm positions, again both representative for the movement tasks of the given parallel kinematic structure.

6.7 WORKING RANGE

The required working range for each arm is defined by the necessary motion angles of each drive train. Exclusively the concept H does not conform to this requirement. The reason is the limitation of the bending angle of the constant velocity joints next to the MAR. The motion angles of the arm around the MAR and the constant velocity joints are calculated through the CAD-System.

6.8 VARIABILITY OF TRANSMISSION RATIO

The predominant part of the concepts has a constant transmission ratio of 70 between the motor and the links. In some concepts the transmission ratio changes depending on the position and orientation of the links. That is because of the two bar linkage, where link 1 and link 2 do not form a parallelogram in the concepts A and E.
For the evaluation the minimum and maximum transmission ratio were calculated numerically and their discrepancy from the target transmission ratio was benchmarked.

6.9 COSTS

The costs of a product are always an important factor. The calculated costs contain the costs for the primary components as well as for purchased parts of a prototype. All these costs were estimated according to the production with conventional lathes and millers (primary components) or requested from suppliers (bearings, gear-wheels, bowden cables etc.). The costs for the servomotors are not considered because they are equal for every concept as they are driven by the same servomotor.

7 EVALUATION

For comprehensive results of the evaluation are displayed in Table 1. The quantitative results from the calculations of the attributes are the basis of the evaluation score. All results were translated to scores between 0 and 10, using linear interpolation between the best and worst attribute value. The concepts F (form fit traction belts in combination with a two bar linkage, score: 8,6/10) and A (parallel motors and a two bar linkage, 8,5/10) are benchmarked highest. The concepts B, C, E and I are not benchmarked much lower (7,7 – 8,1), only the concepts D (serial structure, 6,9/10) and H (constant velocity joint, 4,7/10) do have a noticeably lower score.
As the scores are close to each other for many concepts, it should be noticed that the quantitative evaluation is based on some uncertainties. The calculated values might differ from reality, due to the simplifications mentioned above and inaccuracies in the technical specifications.
Nevertheless, the evaluation results can be used to gain good knowledge of the properties of the robotic structure.
Individual requirements of the manipulator and handling tasks, resulting in different weighting factors, influence the overall score for the concepts and even minor changes can change the ranking order significantly. Therefore, the evaluation always needs to be performed according to the requirements of the manipulator. As an example very good dynamic properties might be important for pick and place applications, while high stiffness and accuracy might be the most important properties in assembly tasks.
For this evaluation, the weighting factors were determined according to the requirements for the PARAGRIP manipulator [1, 2]. They were evaluated using a preference matrix, where the importance of the entire attributes is compared to each other. The count of dominant importance equals the weighting factor. The accuracy and MOI are the most important criteria. In consequence concept F was chosen for the final PARAGRIP manipulator due to its very high

stiffness, low backlash and compact arrangement of the motors resulting in a low MOI.
Concept A does have good properties for most of the criteria, only the variability in transmission ratio is a general disadvantage of the concept. Avoiding this disadvantage in concept B, the MOI and the size ratio are above standard due to the resulting arrangement of the motors. The same is true for concept C, with similar properties. Concept D, using a serial structure, does have a very high MOI and static torque at very low production costs, so it is suitable mainly for tasks with very low dynamic requirements. The properties of concept E are on an average level, with exception of the discrepancy of the transmission ratio. To fulfil the working range, critical transmission ratios in the two bar linkages have to be accepted, which will lead to an exclusion of this concept in most cases. Concept G does have a very low MOI and good overall properties on costs of the stiffness of the system. It might be suitable for high dynamic tasks with low demands in stiffness and accuracy. Concept H does have a number of disadvantages, because of the high number of machine parts and their complex arrangement. Its overall score is going to be very low in most cases. The interlacing of three shafts in concept I leads to a high number of elements, resulting in very high production costs and a high overall mass.
The evaluation shows, that the concepts differ noticeably from each other in their properties and should be chosen dependent on the requirements of the manipulator. An optimal structure for every task cannot be identified.

Table I - Evaluation criteria, Weighting factors, score and evaluation results.

	Concept:	**A**	**B**	**C**	**D**	**E**	**F**	**G**	**H**	**I**
Criteria	**Weighting**	**Score**								
Low compliance	0,19	10	10	10	10	10	10	0	8	7
Low Backlash	0,17	9	9	10	9	9	10	9	0	8
Low Moment of Intertia	0,22	7	5	4	0	8	7	10	8	9
Low Mass	0,06	9	9	9	10	9	8	8	0	2
Low Size Ratio	0,08	7	5	5	8	7	7	10	0	9
Low static torque	0,06	10	10	9	0	9	10	10	10	10
High Working Range	0,08	10	10	10	10	10	10	10	0	10
Low variability of transmission ratio	0,08	7	10	10	10	0	10	10	10	10
Low costs	0,06	7	7	8	10	4	4	3	0	0
weighted Σ	1	**8,5**	**8,1**	**8,0**	**6,9**	**7,9**	**8,6**	**7,4**	**4,7**	**7,7**

8 WEAK POINT ANALYSIS

A weak point in a concept can be identified by scores below standard. They have to be identified and eliminated in concepts with a good overall score, if possible. The analysis visualizes the score of each evaluation criterion including the weighting factor. A weak point analysis is carried out for the concept F (Table II) and concept G (Table III).
The analysis of concept F shows that there is a weak point caused by the relatively high costs. It can partly be eliminated by different cost optimization methods and furthermore the weighting of the criterion is low in this case. The score for the MOI, the mass and the size ratio are only a little below standard, without being a critical weak point.

Table II - Weak point analysis, Concept F.

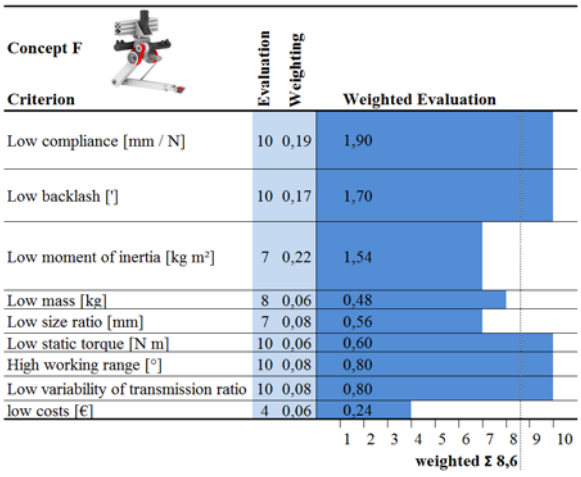

Table III - Weak point analysis, Concept G.

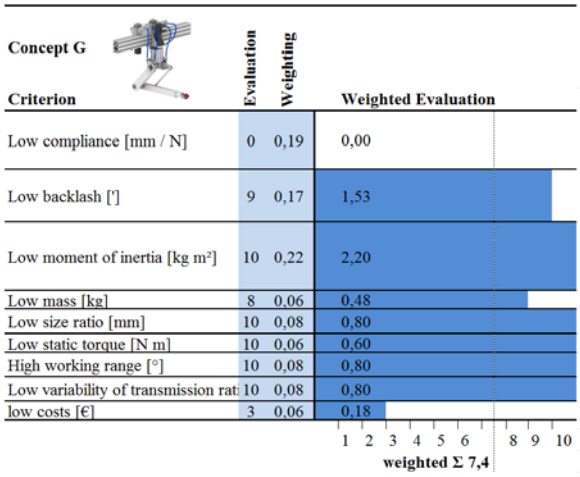

The concept G is a prime example for a weak point analysis. Although the concept in general is evaluated well, it has two weak points. These are the compliance and the costs. The Bowden cables have a comparably low stiffness and the costs are relatively high due to numerous individual parts. The high compliance can hardly be avoided in this concept, which leads to the exclusion of the concept taking into account the existing weighting factors. For the costs the same as for the former mentioned concept is true.

9 CONCLUSIONS

This paper presents a conceptual procedure to obtain and evaluate a set of principle solutions and concepts for the drive train design of the regional structure of a parallel manipulator.

The motor position, orientation and the drive train have great influence to the properties of the robotic structure and a wide range of principle solutions can be obtained from their variation. Their number can be reduced to a reasonable amount by qualitative benchmarking and elimination of solutions that are not feasible in practice. The 9 concepts, resulting from the combination of the remaining solutions, need to be evaluated, according to the requirements of the finally implemented parallel manipulator. 9 quantitative evaluation criteria that can be obtained with adequate effort were developed. They represent the properties relevant for a manipulator. Finally, the evaluation was performed for given requirements, including a weak point analysis. It was shown, that there is no optimal structure for every task and that the best structure according to the individual requirements needs to be identified for the design of a manipulator.

Acknowledgments

As parts of this works are within the scope of the cluster of excellence “Integrative production technology for high-wage countries (EXC 128)”, the authors thank the German Research Foundation for the support.

REFERENCES

[1] Müller, R., Riedel, M., Vette, M., Corves, B., Esser, M., Hüsing, M., *Reconfigurable Self-Optimising Handling System*. Ratchev, S. (ed.) IPAS 2010. IFIP AICT, vol. 315, pp. 255–262. Springer, Heidelberg, 2010. ISBN 978-3-642-11597-4

[2] Riedel, M., Nefzi, M., Huesing, M., Corves, B., *An adjustable gripper as a reconfigurable robot with a parallel structure*. Proceedings of the Second International Workshop on Fundamental Issues and Future Research Directions for Parallel Mechanisms and Manipulators, pp. 253–260, 2008.

[3] Roos, F.; Johansson, H.; Wikander, J., *Optimal selection of motor and gearhead in mechatronic applications*. Mechatronics 2006(16), pp. 63–72, 2006.

[4] van De Straete, H.-J.; Schutter, J.-D.; Belmans, R., *An efficient procedure for checking performance limits in servo drive selection and optimization*. IEEE Trans Mech 1999;4(4), pp. 378–86, 1999.

[5] Choi, C et. al., *A Motor Selection Technique for Designing a Manipulator*. International Conference on Control, Automation and Systems 2007, Seoul, Korea, 2007.

[6] Pettersson, M., *Design Optimization in Industrial Robotics*. Dis., Linköping, Sweden, 2008.

[7] Pettersson, M.; Ölvander, J., *Drive Train Optimization for Industrial Robots.* IEEE Transactions on Robotics, Vol. 25, No. 6, 2009.

[8] Karbasi, H. et. al., *Uni-drive modular robots theory, design, and experiments.* Mechanism and Machine Theory 39, pp. 183–200, 2004.

[9] Lens, T. et. al., *BioRob-Arm A Quickly Deployable and Intrinsically Safe, Light-Weight Robot Arm for Service Robotics Applications.* Proceedings of the 41st International Symposium on Robotics (ISR 2010), pp. 905-910, 2010.

[10] Kurtenbach. S.; Detert. T.; Riedel. M.; Hüsing. M. and Corves. B., *Motor positioning and drive train design for a 3-DOF robotic structure.* New Trends in Mechanisms and Machine Science, Springer Verlag, 2013.

[11] VDI-Fachbereich Produktentwicklung und Mechatronik, *Design engineering methodics - Engineering design at optimum cost - Valuation of costs.* in VDI 2225 Blatt 3, Beuth Verlags GmbH, Berlin, 1998.

ISSN 1590-8844
International Journal of Mechanics and Control, Vol. 14, No. 01, 2013

ON THE FLY PICKING OF PARTS IN A METALLURGICAL MANUFACTURING CELL

Nick Andrei Ivanescu* Liviu Ciupitu* Mihai Parlea** Sorin Brotac**

* University Politehnica of Bucharest
E-mail: nik@cimr.pub.ro, liviu.ciupitu@omtr.pub.ro

** S-ind Process Control S.R.L.
E-mail: mihai.parlea@s-ind.eu,sorin.brotac@s-ind.eu

ABSTRACT

This paper presents a low-cost way of integrating on the fly robot part picking by using machine vision in the metallurgical field. This solution eliminates the expensive software and belt encoders by means of careful workspace planning and high accuracy belt speed control by using a frequency converter. The paper shows the needed calibrations in order to achieve this goal, calibrations that are in fact hidden behind training wizards on the expensive software. This is enabling people with medium knowledge in the field of robotics to achieve high yield industrial on the fly part picking at prices that do not include expensive software or prone to failure belt encoders.

Keywords: Industrial Robots, Robot Vision, Manufacturing Cell Control

1. INTRODUCTION

The majority of local and international economical agents invest large sums in production automation and management without which subjects such as performance and quality cannot be discussed. More and more companies are developing departments for implementing modern automation solutions and computer systems for implementing hierarchic control [11], [12].
Implementing high productivity is the main objective of the companies administration councils plans drawn for the manufacturing process refurbishment and modernisation. The aim of this research is to develop and test a model for results validation so that fallowing validation this technology will globally be implemented on all equipment and manufacturing cells.

Contact author: Nick Andrei Ivanescu

University Politehnica of Bucharest, Faculty of Control and Computers, Spl. Independentei 313, Bucharest, Romania

On a global scale robot integration in flexible production cells/lines is more and more common; process customised solutions are being implemented by the leading companies. Extending traditional material handling control to material conditioning allows for both the laxity of constraints imposed by handling and transport systems part of the manufacturing process material flow and for real-time quality control integration in the global manufacturing system [3], [11].
This functional extension of robot - artificial vision architecture coordinated by PLC can be implemented by [13]: a consistent description of the material flow by an efficient set of features such as shape, surface and position for the useful parts based on high speed real time image processing applying artificial intelligence concepts for obtaining a globally and autonomous behaviour of self-learning, self-correcting, task and content based for the robot fabrication process with working environment adaptation which is an integrated part of the global control application for the entire technological process composed of different task that cooperate between them [6], [7], [2].
The robot - vision units represent the intelligent components of the future intelligent autonomous production, transport and storage systems [8].

Currently similar projects are present in various industries such as automobile, electronics and food processing but few projects operate in the metallurgy field; also through this research the performances of such systems will be improved through real time video correction algorithms and through intermediate product inspections [9].
The production control topology used in this research (see Figure 1) is based on the hierarchical systems theory that are characterised by a "master-slave" subordination relation which offers an attractive alternative with a simple management structure that offers a threshold for less monitoring and control and more responsibility and statistics [4].

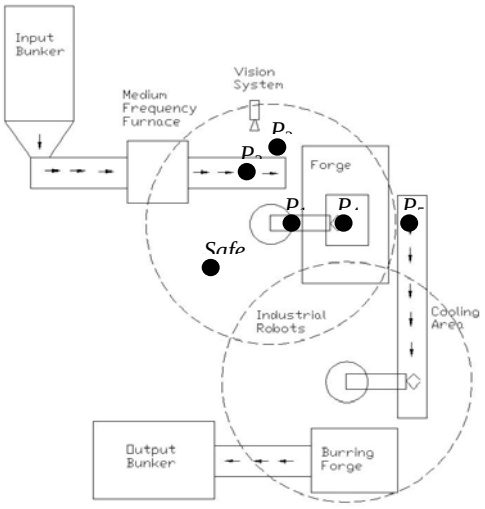

Figure 1 Application scheme

Usually the forged pieces are inserted from a bunker into a furnace in order to be heated (see Figure 1). The hot part comes out from a medium frequency furnace with a random orientation or that can be fixed by special mechanisms, depending of the shape of part.
But because of high temperature of part the individualization and orientation of part is difficult to be made with a good accuracy. So, a vision system to recognize the position of part and to communicate with the robot controller (see Figure 2) in order to make the position and orientation corrections of picking configuration is necessary. [1].

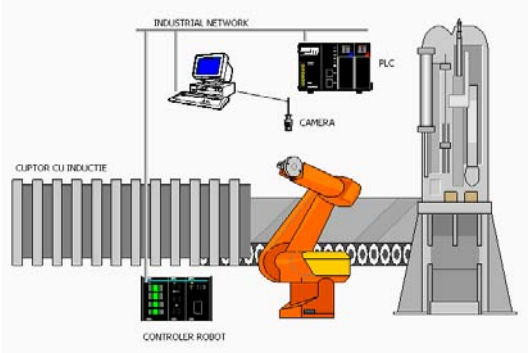

Figure 2 Communication scheme

From delivering port of furnace the part is inserted by lateral into the forge and left down inside the forging mould. The inserting window is relatively small and requires a long link 6 (see Figure 3) or long gripper fingers.
Sometimes another task of spraying the parts of forge is done by the same robot with the aid of a special dose fixed to the robot arm or to the gripper. Anyway, the different planes in which the pick-and-place are done, and the small window of forge where the robot arm must be inserted, impose a 6 DOF spatial mechanism for robot mechanism.

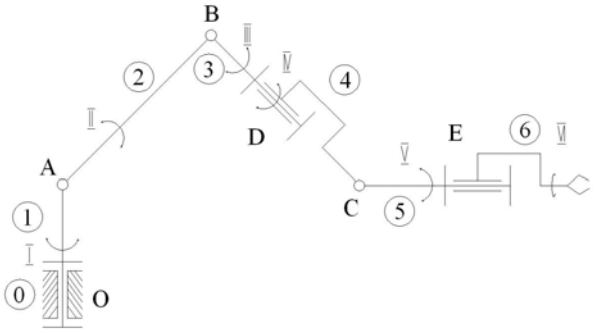

Figure 3 Articulate industrial robot with 6 DOF

An industrial robot with a mechanical structure of cylindrical type with at least 5 DOF may solve the problem too, but the translational joints are pretentiously even in case of cold manufacturing processes.
Actuating system is electric one for robot and pneumatic one for its gripper. The end-effector could be cooled by the aid of a fan or by pressure air in some situations when the temperature of manipulating part is high and the heat cannot be eliminated by the movement of the robot during one cycle.
The same inserting mode is used to put the work piece into the burring forge (see Figure 1). That can be done by another robot or by a human operator, but the work piece should be cold enough to not be deformed when the burring is done. So, a cooling area is interposed between main forge and burring forge, by using some fans. The transfer from main forge to the conveyer can be done by first robot or by the forge mechanism itself.
Finally the forged piece is directed to another bunker and transported to another manufacturing cell.

2. CALIBRATION FOR ON THE FLY PART PICKING

Picking parts on the fly from a moving conveyor is a high productivity and very spectacular industrial application. In this application a vision guided robot coordinates itself with a conveyor and picks parts from it while the conveyor is moving. Since in the real world the coordinates systems from robot, camera and conveyor are rarely aligned (see Figure 4), expensive "Conveyor tracking" software upgrades are available in order to calculate and apply the

needed corrections. Also, the conveyor speed may vary over time due to supply energy variations or wear and tear on the mechanical parts (ac motor, bearings, etc.), this means that usually an expensive encoder is attached to the conveyor in order to keep precise track of its speed.
Since a new workstation that implies pick on the fly is being built, the scope is to apply a strict control on how the equipment is placed in the workstations, this means placing the equipment as close as possible to the ideal state. This requires four sets of calibrations:

1. camera - belt *xy* calibration
2. robot - camera/belt *xy* calibration
3. robot - vision calibration
4. robot - belt speed calibration

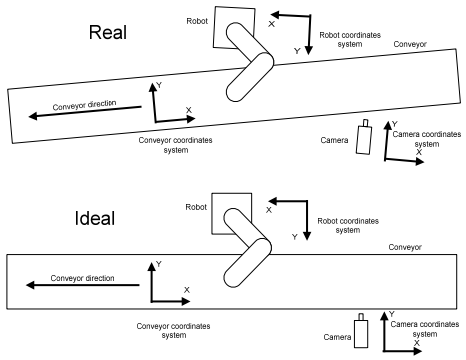

Figure 4 Ideal vs. Real equipment placement

There are two types of camera-to-robot transformations: for *fixed-mounted* cameras and *robot-mounted* cameras. In our case, camera is *fixed-mounted.*
According to [5], the parameters of the scene model can be obtained, during the calibration process, from the following three elementary transformations:

1. *Scaling*: provides the decoupling of the visual information from the image acquisition equipment (CCD camera, lens, frame grabber), with a certain resolution which may vary from one situation to the other according to the camera's mounting. Scaling is necessary because the image taken from a camera has distortions on both *x* and *y* axes.
2. *Rotation*: provides the parallelism between the camera's scaled coordinate system and the reference coordinate system of the robot.
3. *Translation*: superposes the origins of the two coordinate systems, which are now in perfect coincidence.

2.1. CAMERA - BELT XY CALIBRATION

This is made to ensure that the *xy* coordinate system of the camera coincides with the belts *xy* coordinate system. In order to obtain this, the calibration screen from the vision software is used (see Figure 5). On this screen, a grid corresponding to the camera coordinate system is over imposed on the image and then the camera is rotated until this coordinate system is parallel to the belt coordinate system. The "zoom in" function is used in order to obtain maximum precision. Once the calibration is obtained, the current camera position is set firmly into place (the camera mounting plate is attached to the conveyor structure) so that it can never move again relatively to the conveyor.

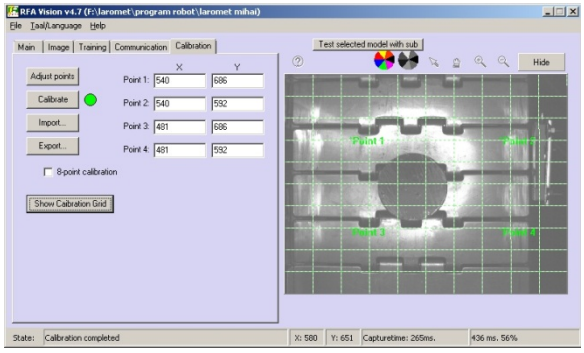

Figure 5 Camera calibration screen

2.2. ROBOT - CAMERA/BELT XY CALIBRATION

With the camera fixed firmly in place relative to the conveyor, the robot gripper is brought into the field of view and is moved along its *y* axis. This motion needs to be parallel to the camera (and so the conveyor) *y* axis, so the whole conveyor is rotated until the movement is parallel to the camera/belt *y* axis. The zoom in function is used in order to obtain maximum accuracy. Once this is obtained, the conveyor structure is fixed firmly to the shop floor.

2.3. ROBOT - VISION CALIBRATION

This is made so that the vision software can obtain the pixel/mm ratio of the camera and that the coordinates generated by the recognition routine are actually the *x*, *y* and rot(*z*) positions that the robot needs to move to in order to pick the detected part. For this the vision software displays four points on the image (see Figure 5), the user needs to move the centre of the gripper in these points and then input the robot *xy* position in the given table (see Figure 6). If the values are equal as in Figure 3 then it means that the first two calibrations have been successful. The Calibrate button is then pressed and the correct calibration if indicated by the green signal next to the button.

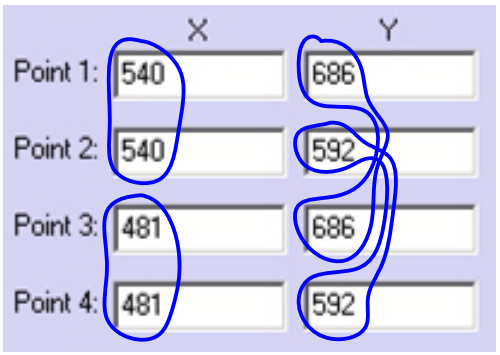

Figure 6 Robot Coordinates for the four points

2.4. ROBOT BELT-SPEED CALIBRATION

The belt is controlled by a frequency inverter so its speed is not influenced by power fluctuation or wear and tear on the mechanical parts. First the frequency inverter is set at a fixed speed, after this the robot is used to measure a segment of the conveyor and then a part is placed on the conveyor and timed as it passes through the designated segment, so the conveyor speed is calculated as:

$$Conv\_speed = \frac{dist}{time} \qquad (1)$$

Then the robot is commanded to move at a set speed along the conveyor for fine tuning. For example, for a frequency inverter frequency of 30Hz a conveyor speed of 73.5mm/s was obtained.

3. ON THE FLY PART PICKING

Now that everything is calibrated, the robot motions necessary for on the fly part picking can be planned. In order to grip the part the robot will have to execute two distinct motions; one for aligning the gripper with the part and one for gripping the part (see Figure 7).

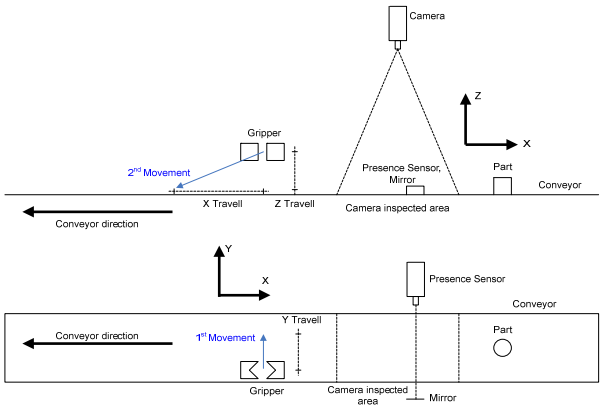

Figure 7 Robot motion needed for part grabbing

3.1. ALIGNMENT MOTION

This motion is used in order to align the robot gripper centre y coordinate with the parts y coordinate so that moving along the conveyor the part will pas directly beneath the centre of the gripper. This motion is started from a fixed known position, the y value that needs to be reached is obtained from the vision software (the x value is not used as this coincides with the park advance along the conveyor and the rot(z) value is also not used as the current part is round) (see Figure 8). The vision sequence has been triggered by the robot in the moment that the part has triggered the Presence Sensor.

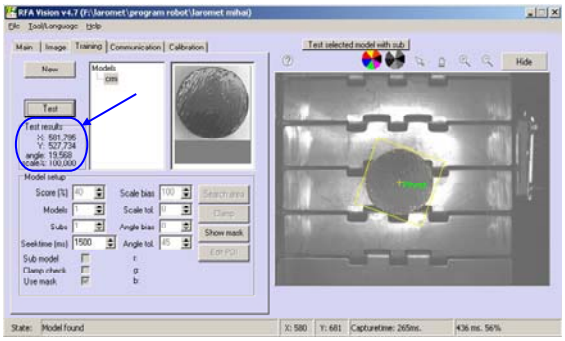

Figure 8 Y value of part position provided by vision software

3.2. GRASPING MOTION

This motion is triggered when the part reaches under the centre of the gripper and is made along the axes x and z in order to lower the gripper fingers on either side of the part without colliding with it; at the end of the motion the gripper is closed so grasping the part. The first problem of this motion is to obtain the start moment, for this, prior to starting the application a part was manually placed in the robot gripper then the robot has been used to measure the distance along the x axis from when the part triggers the presence sensor to the robot starting position (Conv_dist), then the waiting time is calculated as:

$$Wait\_time = \frac{Conv\_speed}{Conv\_dist} \qquad (2)$$

In order to time this period of time, a timer is started when the part triggers the Presence Sensor and this motion will be triggered when this time has expired (meanwhile the vision sequence will have ended and the robot would have executed the Alignment motion).
In order to execute this motion we will need to impose a *Z_travell* sufficient so that the gripper fingers will have descend enough on either part of the part in order to grab it and an arbitrary *X_travell* long enough so that the resulting speed of the motion will not exceed the robot maximum implemented speed. Once this has been determined, the time of this motion is calculated as:

$$Motion\_time = \frac{Conv\_speed}{X\_travell} \qquad (3)$$

Then the robot is commanded to move to the position described as being offset with X_travell and Z_travell along the robots x and z axes. The speed of the motion is set so that the motion is completed in the imposed Motion_time.

4. IMPLEMENTATION

The whole process can be sintetized in the following diagram (see Figure 9):

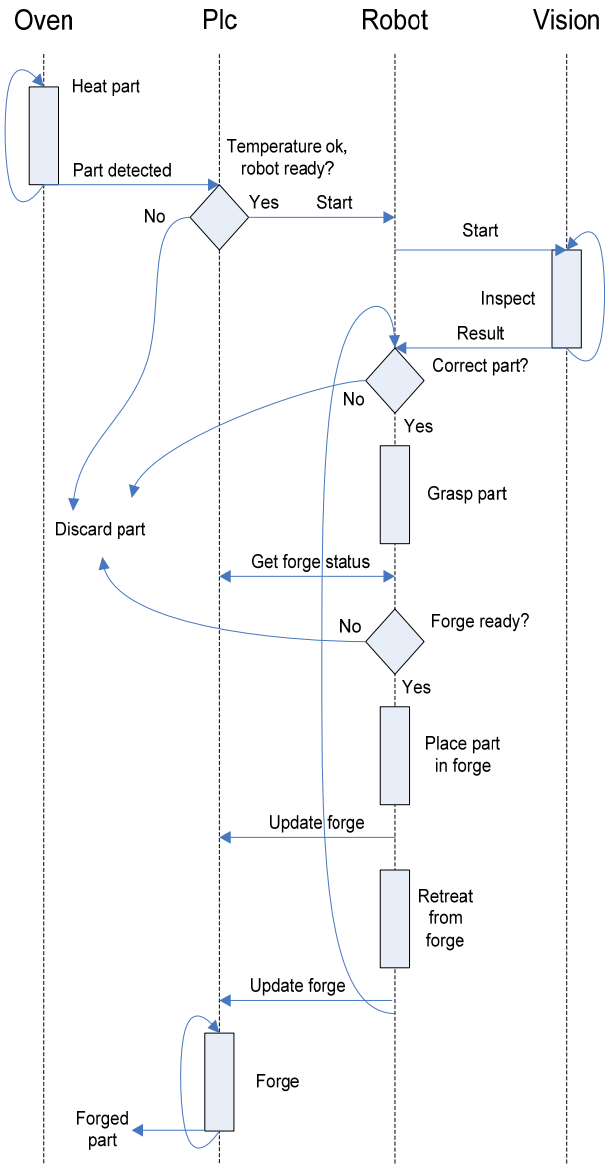

Figure 9 Complete process diagram

The robot controller needs to control the movement of the robot arm, interlock with the Cell Plc and communicate with the Vision Controller. A problem with this controller is that, although it is a multitasking controller, it enables the user to use only two task, a "robot" task that can move the robot and access the communication interfaces a and "process control" task that can only access the communication interfaces. With these restrictions, the robot task will be used for robot movement and interlock with the Cell Plc and the process control task will be used for communication with the vision controller. The hierarchy of the two tasks is based on the Master - Slave hierarchy with the robot task being the Master and the vision task being the Slave.
Data and commands are exchanged between the two tasks using the following data structure:

- Signal 2254 - commands the vision task to open / close the Tcp/Ip connection with the Vision Controller
- Signal 2253 - commands the vision task to execute the vision sequence
- Signal 2252 - the vision task informs that the vision sequence is complete
- Ip/Port - the Ip and Port for communicating with the Vision Controller
- VisStatus - status of the last executed vision sequence, 1 = the sequence was executed successfully and at least one instance of the model was found, 0 = the vision sequence was not executed successfully or no instances of the model were found
- ModelCount - states the start index of the model array from which the vision task will begin to write data for the detected instances, after writing the data the vision task will replace ModelCount with the data index of the last detected instance
- MaxModel - maximum number of instances to be returned by the vision task, after writing instance data the vision task will replace MaxModel with the number of detected instances
- FindModel - name for the model that is to be searched (empty string for any model)
- VisModels - array with the names of detected instances
- VisXVals - array with the x coordinate of the detected models
- VisYVals - array with the y coordinate of the detected models
- VisAngels - array with the rotation angle of the detected models

The Vision Controller runs on the Cell Pc and its task is to analyze the images taken by a camera connected to the Pc via Usb port in order to detect instances of the requested part models. A vision sequence consists of camera settings for grabbing images, a list of learned part models each with its own set of detection settings and robot calibration data. The controller can be directed to search for one particular or for all the models in its list. If the user desires to change any settings then he must do it manually or manually load a different vision sequence.

5. EXPERIMENTAL RESULTS

The system has been implemented in a forge press manufacturing cell (see Figure 10). The role of this cell is to heat blank parts and then forge them. As can be seen in Figure 10, the parts are heated by the induction oven and then placed on the conveyor, where the robot pick them on the fly and places them in the forge. Then the PLC triggers the forge and the finished parts are removed by the sole remaining ironworker (which has also been trained to supervise the whole system).

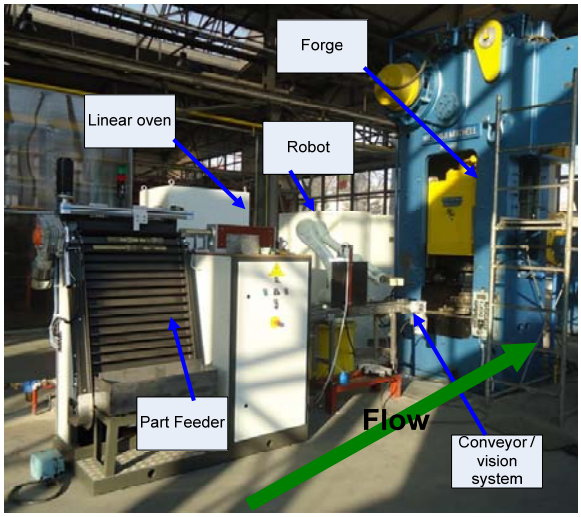

Figure 10 The flexible metallurgical cell

The rate at which the linear oven produces parts is commanded by the PLC. Extensive tests were carried out so that the oven cadence was reduced while the conveyor and robot speed was increased. The robot speed reached its maximum at 60%. Also the belt speed reached 100% of the engine drive (50Hz).
The whole system has been tested and can function at a maximum rate of a part every 7 seconds and can do so indefinitely as opposed to the batch system imposed by the stoker having to manually fill the gas oven with parts and then wait for the whole batch to heat up.

6. CONCLUSIONS

The biggest achievement of this work was the possibility to implement on the fly part picking without a belt encoder and without an expensive belt tracking vision software.
Also, two furnace workers were replaced by the robot resulting in a much more efficient process.
The future work will include learning of other different models of parts and pick them up on the fly.

7. REFERENCES

[1] Ciupitu L., Ivanescu A. N. and Brotac S., Industrial Robots Used in Forge Applications, *Proceedings of 20-th International Workshop on Robotics in Alpe-Adria-Danube Region "RAAD 2011"*, Brno, ISBN 978-1-4244-6884-3, pp. 2038-1 – 2038-6, 2011.

[2] Aissani N., Trenstesaux D. and Beldjilali B., Use of machine learning for continuous improvement of real time manufacturing control system performances, *Int. J., Ind., Syst. Eng.*, 3(4), pp. 474 – 497, 2008.

[3] Babiceanu R., F. and Chen F., F., Development and applications of holonic manufacturing systems: a survey, *Journal of Intelligent Manufacturing*, 17, pp. 111 – 131, 2006.

[4] Barata J., Camarinha-Matos L., M. and Onori M., A Multiagent Based ControlApproach for Evolvable Assembly Systems, *INDIN - 3rd IEEE International Conference on Industrial* informatics, IEEE Explore, Perth, Australia, , pp. 478 - 483, 2005

[5] Borangiu Th., Intelligent Image Processing in Robotics and Manufacturing, Romanian Academy, pp. 75 – 80, 2007.

[6] Borangiu Th., Raileanu S., Rosu A., Parlea M. and Anton F., Management of changes in a holonic manufacturing system with dual-horizon dynamic rescheduling of production orders, *13th IFAC Symposium on Information Control Problems in Manufacturing – INCOM 2009*, Moscow, 2009.

[7] Borangiu Th., Gilbert P., Ivanescu N. and Rosu A., An implementing framework for holonic manufacturing control with multiple robot-vision stations, *EAAI 22 4 – 5*, Elsevier, pp. 505 – 521, 2009.

[8] Borangiu Th., Balibrea T., Anton F., Ivanescu N., Dogar A. and Raileanu S., Holonic fault-tolerant control of networked robot-vision assembly stations, *Intelligent Assembly and Disassembly IAD 2007*, May 23 – 25, Alicante, Spain, 2007.

[9] Borangiu Th., Raileanu S., Ivanescu N., Anton S. and Dogar A., RVHOLON - A holonic Control Platform, *Proceedings of the 3rd National Conference "Cercetarea de Excelenta"*, Brasov, Romania, 2007.

[10] Darmoul S., Pierreval H. and Hajri G., An immune Inspired multi Agent System to Handle Disruptions in Manufacturing Production Systems, *Proceedings of IESM 2011*, ENIM-Metz, France, 2011.

[11] De Ugarte B., Artiba S. and Pellerini R., Manufacturing Execution Systems - A Literature Review, *Production Planning and Controll*, 2009.

[12] Filip, F. and Leiviska K., Large-scale Complex Systems, *Springer handbook of Experimental Solid Mechanics*, hb17-036, 2009.

[13] Ivanescu N., Parlea. M. and Rosu A., Different Approaches Regarding the Operational Control of Production in a Flexible Manufacturing Cell, *1st Workshop on Service Orientation in Holonic and multi-Agent Manufacturing Control*, Paris, 2011.

ISSN 1590-8844
International Journal of Mechanics and Control, Vol. 14, No. 01, 2013

A LOW-COST CONTROL ARCHITECTURE FOR CASSINO HEXAPOD II

Giuseppe Carbone* Franco Tedeschi*

** LARM: laboratory of Robotics and Mechatronics,*
DICEM; University of Cassino and South Latium - Cassino, Italy
URL: http://webuser.unicas.it/weblarm/larmindex.htm

ABSTRACT

This paper presents the design of a low-cost control architecture for an hybrid hexapod walking machine that has been designed and built at LARM: Laboratory of Robotics and Mechatronics in Cassino. Main attention has been addressed to the selection of suitable commercial low-cost hardware components. Then, suitable hardware interface components have been carefully designed and built. Moreover, special care has been addressed in developing a software architecture that can be user-friendly also for non-expert users. Preliminary experimental tests have been reported in order to show feasibility and operation capability of proposed design.

Keywords: Design, Walking Machines, Low-Cost Control

1 INTRODUCTION

The design of walking machines is a challenging topic that has attracted the interest of many researchers. Several designs of walking machines have been proposed, for example for demining, pipe inspection, inspection and restoration of archeological sites, and interplanetary exploration as reported in (Berns 2007; Salmi & Halme 1996; Gonzalez de Santos et al. 1998; Horodinca et al. 2002; Zielinska & Heng 2002).

Mobile robots can be structured of different types, first ones are based on crawlers or wheels and second ones are equipped with biologically inspired legs. This second type of walking machines can be slow and more difficult to design and operate with respect to the first ones. Nevertheless, legged robots are more suitable for rough terrain, where obstacles of any size can appear (Carbone & Ceccarelli 2004). In fact, the use of wheels or crawlers limits the size of the obstacle that can be climbed to half the diameter of the wheels (Chakraborty & Ghosal 2004). On the contrary, legged machines can overcome obstacles that are comparable with the size of the machine leg (Carbone & Ceccarelli 2005). There is also a third type of waking machines that is called hybrid robot, since it has legs and wheels at the same time.

Contact author: Giuseppe Carbone[1], Franco Tedeschi[2]
[1] carbone@unicas.it
[2] franco.tedeschi@unicas.it
A preliminary version of this paper has been presented at RAAD 2012 Conference in Naples.

This type of walking machines may range from wheeled devices to true walking machines with a set of wheels. In the first case, the suspensions are arms working like legs to overcome particularly difficult obstacles, and in the second case, wheels are used to enhance the speed when moving on flat terrain.

This paper reports the design of a low-cost control architecture for a novel hybrid walking machine that has been designed at LARM as an evolution of the Cassino Hexapod robot (Carbone et al. 2007). This hybrid walking machine is composed of six legs having a modular anthropomorphic architecture with a wheel at its extremity as shown in Fig. 1.

Figure 1 A built prototype of Cassino Hexapod II.

Main attention in the process design of mobile robot system has been addressed to the selection of low-cost hardware components. Moreover, a suitable user-friendly software architecture has been developed also for non-expert users. Expected field of application for this prototype can be the inspection and operation in non-accessible sites, as outlined in (Cigola et al. 2005).

2 HARDWARE ARCHITECTURE

The operation of the proposed novel six-legs hybrid walking machine requires the following minimum set of components as also shown in the scheme of Fig.2

- 18 motors (3 for each leg);
- 18 encoders (one for each motor);
- connection cables for each motor;
- 6 wheels;
- a control board;
- a camera and/or additional external sensors;
- an user-interface;
- a power supply;
- a software library for various operation modes.

Motors can be of several different types. Considering the small size of the proposed prototype, the most convenient choice are the DC servomotors. In fact, this type of motors is widely available on the market. Usually, it has a relatively small size and can be purchased at low cost.

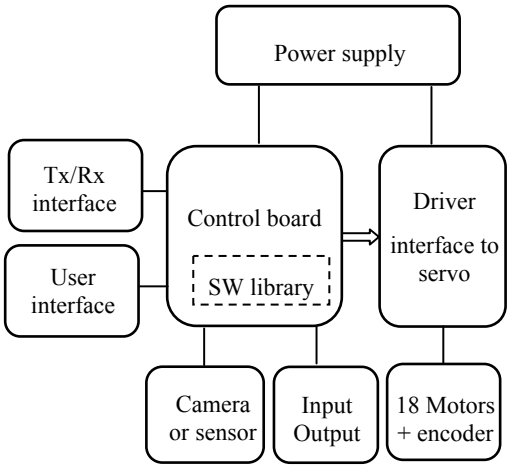

Figure 2 A scheme of main control architecture components for the proposed system.

2.1 SERVOMOTORS

A servomotor is composed of an electric motor, a reduction gearbox, a position feedback system for the axis output, and an electronic control for close-loop positioning of the output. The control of the servomotor is achieved by means of a proper duty cycle PWM modulation. Figure 3 shows an exploded view of a servomotor with its main components (Servocity, 2012). The main features of the standard servomotor in Fig.3 (HITEC model HS-322HD) are:

- Input power voltage from 4.8 V to 6 V;
- Output torque from 0.3 to 0.37 Nm ;
- Output axis rotation from 0 to 180 deg.;
- Operating speed from 0.15 to 0.19 sec/60 deg. at no load;
- PWM pulse signal ranging from 0.6 ms to 2.4 ms;
- Idle current from 7.4 mA to 7.7 mA;
- Running Current from 160 mA to 180 mA at no load;
- Dead band width 5μs;
- Weight 0.043 kg.

The output shaft of a standard servomotor usually can rotate from 0 to 180 deg.. This rotation range is suitable for actuation of leg joints of the proposed hexapod robot. But, the rotation of wheels requires a continuous rotation of the input axis: a modified servomotor is required for this purpose. The main features of the commercial continuous rotation servo adopted (Parallax mod 900-00008) are:

- Input power voltage from 4.8 V to 6 V;
- Output torque from 0.27 Nm ;
- Output axis speed from 0 to 50 RPM.;
- PWM pulse signal ranging from 1.3 ms to 1.7 ms;
- Weight 0.043 kg.

Only close-loop speed control is possible for this type of servomotors in both clockwise or counterclockwise directions. The above-mentioned motor is suitable for the operation of the wheels. The angular position of each wheel can be obtained by a proper software routine.

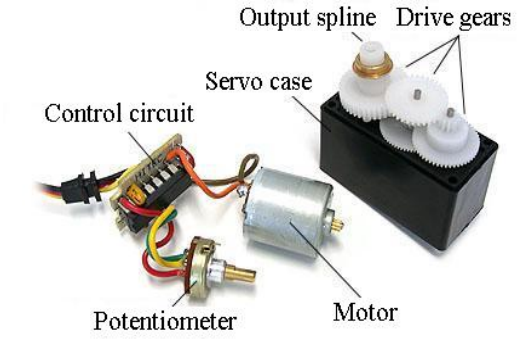

Figure 3 A photo of a commercial servomotor with main components (Servocity, 2012).

2.2 MECHANICAL DESIGN

The proposed design has been conceived for developing a walking leg by using mainly low-cost components with the following basic requirements:

- to have a robust simple mechanical design;
- to have a modular design that can be used for robots with different number of legs;
- to be operated with an easy flexible programming;
- to have low-cost both in design and operation.

Those requirements can be achieved in a very practical way by using low-cost components from the market into a suitable design for the whole system.
The leg body is composed of links made of POM (Polyoxymethylene), a commercial thermoplastic having high stiffness, low friction and excellent dimensional stability. POM has a density of $\rho = 1.42$ g/cm^3, tensile strength 70 N/mm^2, modulus of elasticity in traction 3000 N/mm^2. Other POM advantages are high abrasion resistance, high heat resistance, low water absorption.
Figure. 4a) shows a detail of main components that have been designed for assembling a robotic leg having two degrees of freedom (dofs). This assembly solution has been designed as based on previous experiences that are reported in (Carbone & Ceccarelli 2004; Carbone et al. 2005; Cigola et al. 2005; Shrot 2006). It is worth noting that the leg is composed of two link. Each module contains two commercial servomotors; the servo output shafts are used in order to connect a module to another one. Additional components are needed for the extremity modules. In particular, the support motor requires additional fixing parts in order to connect the leg to the robot body, and the leg extremity link requires an additional wheel. The described leg has a total height of 0.2 m and a weight of about 1.5 N; its maximum step size is of 50 mm. It is worth noting that legs having more dofs can be assembled by adding more modules. The above-mentioned modular design of one leg has been used as basic component for the Cassino Hexapod II. In particular, six legs have been connected to a suitable body in order to build the prototype shown in Fig.4b).This walking machine can fit into a cube of 0.4 x 0.25 x 0.2 m^3 and it has an overall weight of 18 N. It can carry on-board its own control board and a pay load of 4 N; in this case, the robot weight is about 22 N. The diameter of wheels is 0.066 m.

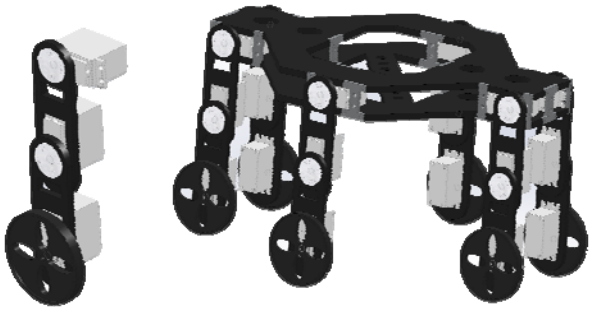

a) b)

Figure 4 a) 3D CAD model of the proposed leg b) A 3D CAD model of the new Cassino Hexapod II

2.3 CONTROL BOARD

A suitable commercial low-cost control board should be capable of operating at least 18 servomotors. Additionally, it should have a significant number of extra Inputs/Outputs for managing additional external sensors and motors in a modular architecture. Arduino ATmega 2560 can be sees as a suitable choice having the above-mentioned features.
In particular, Arduino ATmega 2560 has:

- 54 GPIO pins, whose 14 can be used for PWM;
- 16 analogic inputs;
- a flash memory of 128 kbytes;
- an EEPROM chip of 4 kbytes;
- a serial I/O port;
- a clock speed of 16 MHz;
- a USB port that can be used also as power source;
- an adapter for external DC power source.

The Arduino ATmega 2560 board, contains all the hardware components for the operation of the embedded microcontroller. It is based on an open-source multi-platform integrated development environment that can be operated via Linux, Apple Macintosh and Windows. This feature allows an user-friendly software implementation of many different customized input/output operations.
The programming of the Arduino can be achieved by means of source codes written in C/C++. The firmware for Arduino operation needs to define two main functions:
setup () - a function invoked once at the beginning of a program that can be used for the initial settings;
loop () - a function called until the card is turned off.

2.4. USER INTERFACE AND POWER SUPPLY

The hardware architecture can be operated via a control console and a joystick. In particular, each buttons selection on the control console in Fig. 5a produces a different types of gaits. The joystick is used for robot driving on flat terrain in a wheeled mode.
The adopted matrix keypad with 12 keys is shown in Fig. 5a: the terminal pins of columns X1,X2,X3, and row Y1,Y2,Y3,Y4 are directly connected to 7 digital input of Arduino. The adopted low cost joystick controller is shown in Fig. 5b. The joystick works in analogic mode: directional movements are two potentiometers - one for each axis. The potentiometers output are connected at two analogic inputs of Arduino control board, they allow to select the forward, backward, turn right, turn left wheeled operation modes.
The power supply of the selected control board and servomotors needs to provide Vcc = 5V and Imax = 4A. A lithium battery with V_{DC} = 11.1 V and 2100 mAh with LM7805 voltage regulator has been selected to cover robot system power needs.

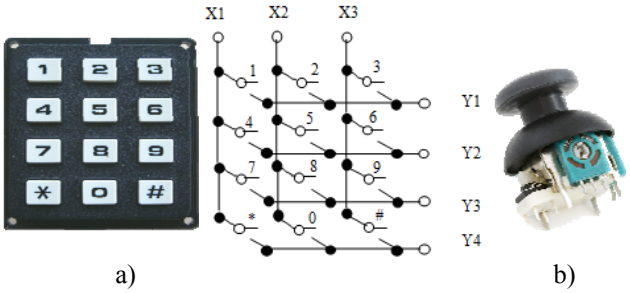

a) b)

Figure 5 The developed user interface: a) a commercial matrix keypad and logical pin-out; b) a low-cost joystick

2.5 DESIGN OF A SUITABLE SERVOMOTOR INTERFACE

One of the main design issues is related with the development of a proper interface between servomotors and the Arduino ATmega 2560 control board. A design solutions implemented and tested is outlined in the scheme of Fig. 6. It provides a direct connection of each servomotor to a digital output port of the Arduino control board. Each servomotor has to be connected to an external power supply, since Arduino cannot provide currents totaling more than 400 mA. The number in the rectangle are the corresponding Arduino digital output pin.

The direct drive mode is the most simple and economical way to drive servomotors with Arduino control board. This solution has been tested by developing a specific board (shield) for the Arduino control board.

Figure 7 shows the built board for the direct drive of 18 servomotors. The geometrical size of the proposed direct drive Arduino shield have been defined to fully match with Arduino Mega 2560 control board pin-out as shown in Fig.7a). Attention has been addressed to the cross sections of the printed circuit board has been set up to be compatible with the needed high currents of the servomotors. Figure 7b) shows the top side of the built direct drive Arduino shield with the connectors to the 18 servomotors and the cable for the external power supply.

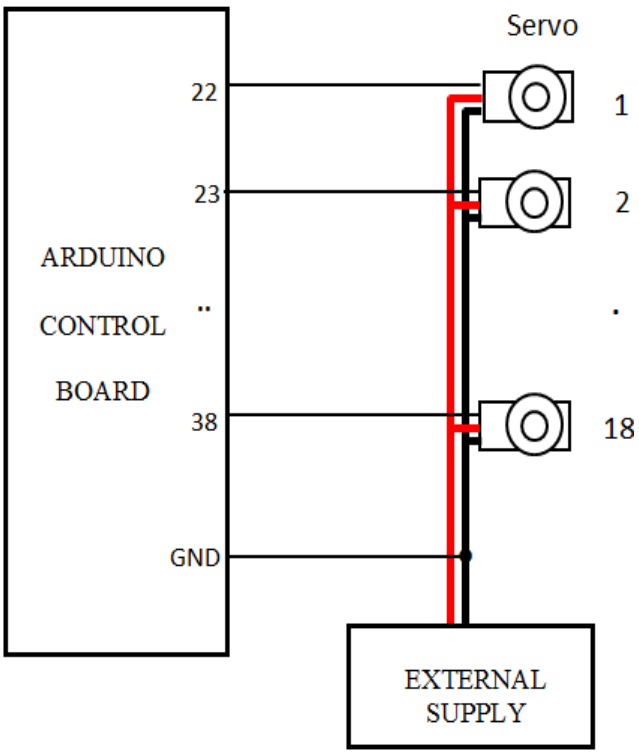

Figure 6 Electrical scheme of the direct drive operation of 18 servomotors with Arduino control board.

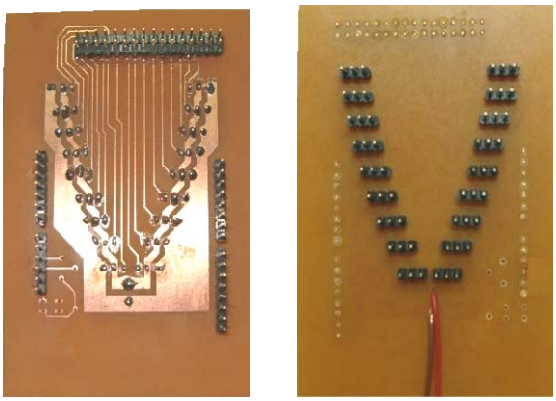

a) b)

Figure 7 A direct drive Arduino shield built at LARM: a) bottom side to Arduino; b) top side to servomotors.

3 SOFTWARE DEVELOPMENT

The Arduino development environment contains a text editor for writing code, a message area, a text console, a toolbar with buttons for common functions, and a series of menus. It connects to the Arduino hardware to upload programs and communicate with them. The operation of the proposed control architecture has been achieved by developing a proper firmware of Arduino control board, as based on the Arduino Servo library. This Servo library provides features for a user-friendly operation of up to 48 servomotors without requiring any setting of PWM.

Figure 8 shows the flow-chart sequence for managing the Servo library for experimental operation tests of servomotors.

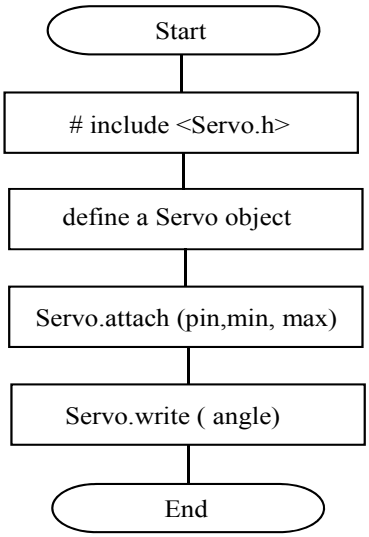

Figure 8 Flow-chart for the servomotor operation.

The first step is to include the Servo library (header file) in the proposed Arduino project. The second step is to define a Servo object. In the third step the attach() function allows to connect the servo object to a specific pin of the Arduino

control board. Moreover, one can define the min parameter that is the pulse width (in microseconds) that is related with the minimum angle of the output shaft position. One can also define the max parameter that is related with the maximum angle of the output shaft position (180 deg.). The last step is the write( ) function. This function sets the angular position of a standard servo (in degrees) so that the corresponding servomotor moves its shaft to this angular position. In the case of continuous rotation servomotors the write( ) function will set the desired speed of the servomotor. In this case a value 0 refers to a full-speed in clockwise direction; 180 refers to a full-speed in counterclockwise direction; 90 refers to a standstill configuration. Two types of movements are being developed with the new Cassino Hexapod II: tripod gait and hexapod gait given by one leg in contact with the floor.

Figure 9 shows a schematic diagram of this types of movement that are being developed. In particular, the figure shows a scheme with movements of six legs also with a footfall formula representation. The legs that are in contact with the ground surface are indicated as black circles in a table in which the entries represent the possible foot contacts with the ground. Fig. 9a) shows a scheme in which the hexapod gait is given by one leg in contact with the floor and Fig. 9b) shows a scheme in which the hexapod gait is given by three legs in contact with floor. In a tripod gait, the front and rear leg of one side and the middle leg of another side perform their swing movements at the same time. Thus, the swings of right and left tripods have to be synchronised by properly setting a time delay among the leg swings.

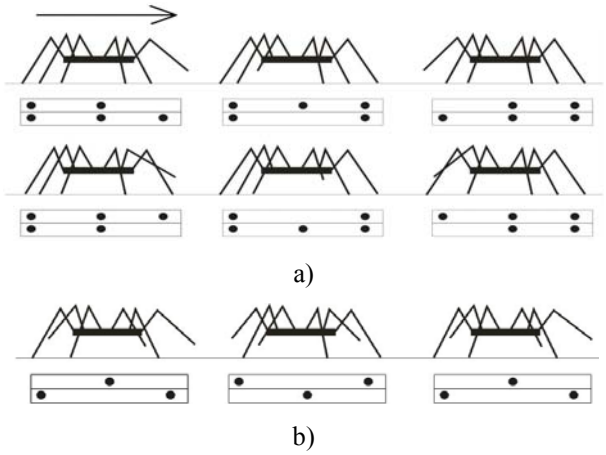

Figure 9 Footfall formulas representation of movements for six legs: a) one-legs gait; b) three-leg gait. (Black circles stands for the legs in contact with the ground surface; arrow indicates the moving forward direction).

4 PRELIMINARY EXPERIMENTAL TESTS

The developed driver card and the firmware for preliminary experimental tests of control board allow to interface and operate 12 servomotors and 6 continuous rotation servos. The overall hardware can be controlled via a control console with 12 keys and a joystick (Fig.5). In particular pushing buttons obtains several types of gaits, while the joystick are used for robot driving in a flat terrain in a wheeled mode. Figure 10 shows a customized module that has been used during servomotor operation tests for measuring the required currents. This board is a carrier of Allegro's ACS712 Hall effect-based linear current sensor.

Figure 10 Customized module for servo current measurement (Sparkfun 2012).

An acquisition card NI USB-6009 (NI webpage 2012) has been used to acquire ACS712 analogic outputs. This acquisition card has been managed within Labview environment. Operation tests have been carried out by using a sweep function (for cycle) that allows direct control the angular position of leg servos from 0 to 90 deg in steps of 1 deg..

Both no load and full load conditions have been tested. Similar tests have been carried out for the continuous rotation servomotors under both minimum and maximum speed values conditions. Experimental results of servo current measurements in various operation conditions show that the required currents by the servomotors are related with the required output torque. Peak current values (I) are required in correspondence of the command tension pulse (V) as shown for example in Fig. 11.

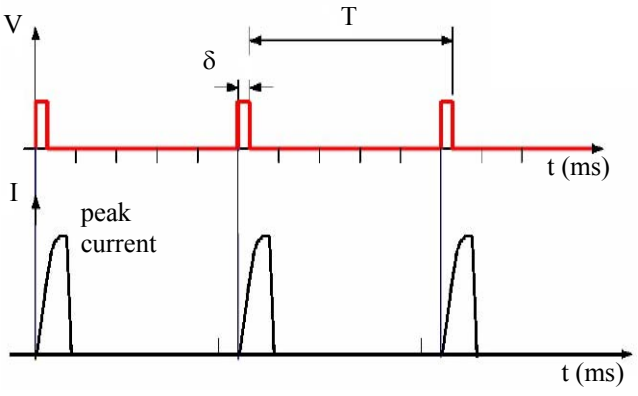

Figure 11 Waveform of the absorbed servo currents.

Table I reports the values of the experimental peak current that have been measured in various operating conditions. All the measured values are within the feasible operation ranges of the selected servomotors.

Table I – Measured values of experimental peak currents.

Servo Group	Peak operating current (mA)
Single Leg	350
Single Leg + load 1.5 N	980
Tripod gait	3000
6 wheels (max speed)	1100

Figure 12 shows a single leg that has been used for the experimental tests. In particular, Fig.12a) shows a front view; Fig.12b) shows a side view with detail of the link joint; Fig.12c) shows a front view with the knee joint at 90 deg. configuration.

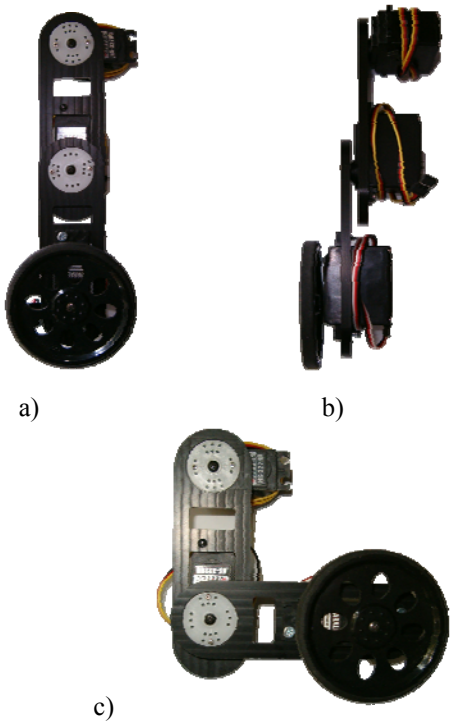

a) b)

c)

Figure 12 A leg prototype: a) front view;
b) side view with detail of link joint;
c) front view with joint at 90 deg. configuration.

CONCLUSIONS

This paper describes a control architecture that has been developed and tested for the Cassino Hexapod II robot that is based on proper low-cost commercial components. The proposed architecture has required the design of a proper servomotor control shield and a user-friendly software library that allows the operation of the required 18 servomotors just by using a matrix keypad and a joystick. Preliminary experimental tests show the effectiveness of the proposed control architecture being all the measured current values within the feasible operation ranges of the selected servomotors. The feasibility of the proposed new design and easy operation modes have been tested experimentally. Results have shown a robust system operation, with limited power consumption, with even lower power consumption is obtained in wheeled operation modes as suitable gait planning. A hybrid robot Cassino Hexapod II can also use wheels for locomotion on flat ground. This way robot can move fast without consuming a lot of energy. Results of the experimental test also demonstrate that commercial lithium batteries can provide a suitable power supply to Cassino Hexapod II for at least 30 minutes continuous operation.

REFERENCES

[1] Arduino homepage, http://arduino.cc/en/Reference/, 2012.

[2] Burkus E., Odry P., “Autonomous hexapod walker robot Szabad(ka)”, SISY 2007, 5th International Symposium on Intelligent Systems and Informatics, Subotica, Serbia, 2007, pp. 103 – 106.

[3] Carbone G., Ceccarelli M., “Legged Robotic Systems”, Cutting Edge Robotics ARS Scientific Book, Wien, pp.553-576, 2005.

[4] Carbone G., Shrot A., Ceccarelli M., “Operation Strategy for a Low-Cost Easy-Operation Cassino Hexapod”, Applied Bionics and Biomechanics, Vol.4, N.4, pp.149–156, 2007.

[5] Horondica M., Doroftei I.,Mignon E., Preumont A.,”A simple architecture for in-pipe inspection robots” International Colloquium on Mobile and Autonomous Systems, Magdebugr, 2002.

[6] LARM homepage, http://webuser.unicas.it/weblarm/larmindex.htm, 2012.

[7] National Instruments webpage “USB 6009”, http://sine.ni.com/nips/cds/view/p/lang/it/nid/201987, 2012.

[8] Nava Rodríguez N.E., Carbone G., Ceccarelli M., Moreno Lorente L.E., “Design Evolution of Cassino Hexapod Robot”, 10th Biennial ASME Conference on Engineering Systems Design and Analysis ESDA2010, Istanbul, paper n. ESDA2010-24020, 2010.

[9] Sparkfun webpage “ACS712” https://www.sparkfun.com/products/8882, 2012.

[10] Sevocity homepage, http://servocity.com/, 2012.

[11] Silva M,F, Machado J.A.T., “A historical perspective of legged robots in Journal of Vibration and control, Vol.13, n.9, 10mpp. 1447-1486, 2007.

[12] Wang Z.-Y., ding X.-L., Rovetta A., “Structure Design and Locomotion Analisys of a Novel Robot for Lunar Exploration”, 12th IFToMM Word congress, Besancon, 2007.

[13] Zielinska T., Heng J., “Development of a walking machine: mechanical design and control problems”, Mechatronics, Vol 12, n. 5, pp 737-754, 2002.

ISSN 1590-8844
International Journal of Mechanics and Control, Vol. 14, No. 01, 2013

MODELLING AND SIMULATION OF A GRIPPING DEVICE FOR OBSTACLE REMOVING ON LUNAR SOIL

Giuseppe Carbone[*] Costantino Falchi[†]
Andrea Manuello Bertetto[†] Marco Ceccarelli[*]

[*]*LARM: laboratory of Robotics and Mechatronics,*
DICEM; Università di Cassino e del Lazio Meridionale, Cassino, Italy

[†]*Dipartimento di Ingegneria Meccanica, Chimica e dei Materiali,*
DIMCM; Università di Cagliari, Cagliari, Italy

ABSTRACT

This paper describes main design issues towards the realization of a grasping prototype that can be used on a rover for removing rocks and debris from the lunar soil. The proposed gripper design is aiming to avoid a dedicated actuation for optimising reliability and minimising weights. For this purpose, a passive grasping operation is proposed by using the available motion capabilities of a lunar rover. Design constrains have been analytically formalized and suitable sizes have been selected for the proposed grasping mechanism. The proposed design solution has been implemented as a multi-body model within MSC.ADAMS environment for numerical validations of its kinematics and dynamic behaviour.

Keywords: Lunar Rover, Gripping system, Simulation.

1 INTRODUCTION

Over the past decades has intensified the focus by the major space agencies toward our satellite. The policy of the world space agencies is focused to exploitation of what is outside the Earth's atmosphere, so as to provide, for 2020, the construction of a lunar base, which will serve as a scientific outpost and launch base for future deep exploration of the universe (Benaroya H. et al., 2002), (Benaroya H. et al., 2008), (Johnson S.W. and Wetzel J.P., 1988).
One advantage of the Moon in this direction is represented by its gravitational field, relatively weak, which makes it easy to throw objects toward the Earth or other destinations. Given the real possibility of realize scientific outposts on other celestial bodies, there is urgent need provide a mechanical support to the crews, through the use of automatic machinery, capable of performing tasks that man is unable to perform, saving time and energy. It is necessary to prepare a portion of the lunar soil, for the construction of the base, removing the rocky debris scattered on the lunar surface. Are being studied new rovers, different from their predecessors, designed to make it easier in the near future the construction of settlements outside of our planet. One of the most successful gripper type is the two finger hand. Mechanical grippers having two fingers are widely used for achieving grasping and handling of specific objects (Pham D.T. and Heginbotham W.B., 1986), (Ambu R. et al., 2010), (Manuello Bertetto A. and Ruggiu M., 2003). However, multi-fingered robotic devices and hands are being also widely investigated, as reported in (Iberal T., 1997) (Dechev N. et al., 1999), (Venkataraman S.T. and Iberall T., 1989), (Ceccarelli M., 2004).
This paper, focuses on issues related to the manipulation of objects in the context of space robotics. The aim is to improve the ability of robots to manipulate objects of different shapes and masses. This type of problem occurs in all those occasions where robots have to operate in special environments, moving objects very different from each other in terms of mass and geometry, and you do not have the opportunity to replace the end effector. This raises the need to provide the robot manipulators, able to self-adapt to the various forms the object to be grasped.

Contact authors: Giuseppe Carbone[1], Andrea Manuello Bertetto[2]

[1] Via G. Di Biasio, 43, 03043 Cassino (Fr), Italy
E-mail carbone@unicas.it
[2] Piazza D'Armi, 09123 Cagliari (Ca), Italy
E-mail: andrea.manuello@unica.it
A preliminary version of this work has been presented at RAAD 2012, 21th International Workshop on Robotics in Alpe-Adria-Danube Region.

2 THE WORKING ROVER

The soil of the Moon is covered with rocks and debris, coming from innumerable meteorite impacts that have characterized the surface of the satellite. Before the construction phase of human settlement, it is necessary to remove the debris in the area chosen for the building base. It is clearly inappropriate to entrust to the human action the heavy task of removing obstacles in lunar environment. Recently, a new concept of space rover has been devised which differs from the predecessors for the tasks assigned. In fact, this rover is mainly assigned to working operations such as the movement of weights to clear from obstacles and arrange the lunar soil, the assemble lunar bases, which will be used as base field for the exploration of the deep space. For these tasks an interesting recently proposed solution is to provide a system consisting of swarms of controlled collaborating working robots. In this paper is presented a gripper on board of a working rover devoted to the described tasks.
The working rover is designed to grab and lift objects with a weigh up to 800 N about, corresponding to a mass of about 500 kg in lunar gravity.

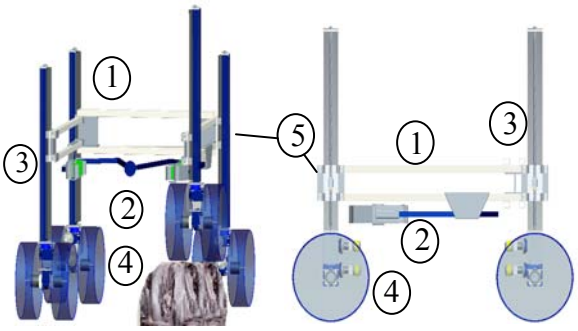

Figure 1 A CAD Model of the Working Rover.

The main features of this lunar rover can be summarized in: gripping operation, lifting load and advancing and arrangement phases. This vehicle has several degrees of freedom and each column is motorized to achieve a linear motion, to move and to control the attitude which can be set to keep a defined plane, independently from the contour of the soil. In particular, each leg of the rover has been designed to allow the motion, the lift, the attitude control of the vehicle.
A scheme of the worker rover is shown in Fig. 1. The frame (1) of the rover is linked to a gripper mechanism (2). Four columns (3), with motorized twin wheels (4), transmit the load to the frame by means of slides (5), which are assembled to the frame The in plane overall rover dimensions are square having a 1,2m side.

3 PROPOSALS FOR A GRIPPER DEVICE

In the following three gripper systems have been proposed as based on planar mechanisms. The proposed grasping mechanisms allow to grasp solid objects, with a generic geometry, as are the numerous lunar masses on the moon surface. This performance comes from the auto adaptability of the grippers to a generic object shape and position. The contact points to sustain the grasped object are always three, to have a securely grasped object.
The first system uses the principle of the articulated quadrilateral. Structurally, it consists of a bumper equipped with hinged rod (1) that can rotate around a pivot point (O), two holding devices (2), two articulated quadrilaterals (3) which are the rover's arm. Two rods (4) connect the arms with the rod bumper (Fig. 2).
The second gripping scheme consists of a mechanism, as shown in Fig. 3, having a bumper member which is the first element that comes in contact with the object. The object, pushing the bumper moves the arms of the gripper. This scheme is more simple that the before described: the mass and the arms number are reduced and there are not sliding but only hinges to connect the gripper arms together and to the frame.

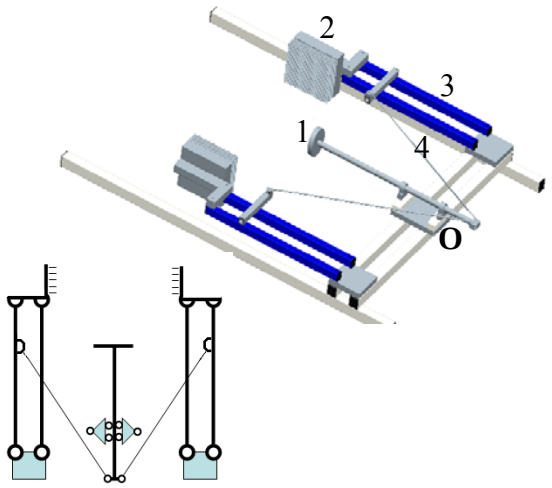

Figure 2 A first gripper mechanism and its scheme.

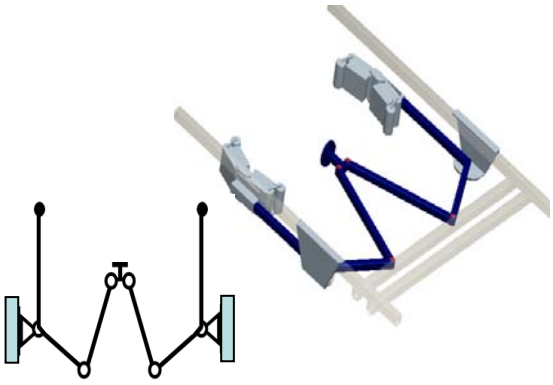

Figure 3 A second gripper mechanism and its scheme.

The third proposed gripper scheme has a geometric scheme like the second one, achieving that the mechanism work space is all in the overall rover frame region. The scheme is represented in Fig. 4.

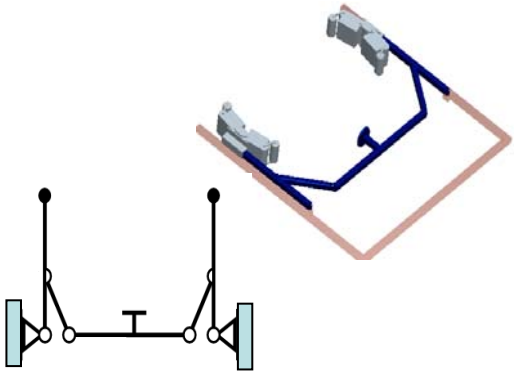

Figure 4 A third gripper mechanism and its scheme.

4 A GEOMETRIC MODEL

The second (and third) gripper scheme is a planar articulated mechanism with three degrees of freedom. This scheme allows to grasp solid objects having undefined shape and also not centred objects. Moreover, a passive grasping operation can be achieved by using the available motion capabilities of the lunar rover.

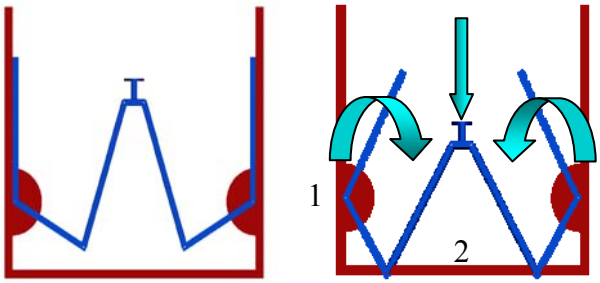

Figure 5 The grab movement.

By a locking system on the of the arms (1) hinges (see Fig. 5), will be possible to achieve stability of the socket object, which can be lifted and moved. During the grasping phase the rover moves against the object leading to close the gripper mechanism on the object, once the object is grasped it is lifted and moved on the Moon soil. Referring to a conventional spherical object shape, the bigger grasping object has a mass of 485 kg on the Moon, corresponding to a sphere having a diameter of 0.65m. This object has a weight of 785N on the Moon, corresponding to a mass of 80 kg on the Earth. These data are referred to a gravity acceleration of 1,6 m/s^2 and of 9,81 m/s^2 on the Moon and on the Earth respectively, and for a lunar rock density of 3345 kg/m^3.

The gripper mechanism is able to grab objects of different shapes and to perform the object grasping in a generic position, also not centred respect to the rover symmetry vertical plane AA in Fig. 6.

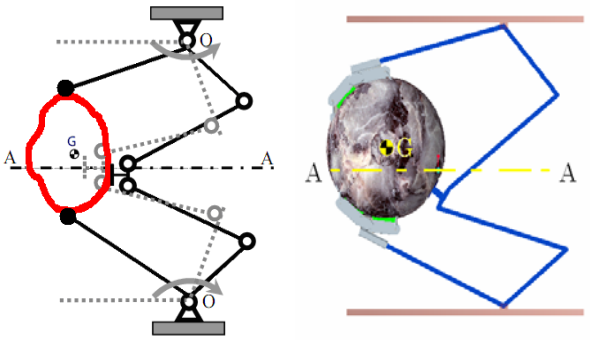

Figure 6 Kinematics and configuration of grasping.

A grasp without interference between mechanism and rover frame can be realised defining the parameters shown in Fig. 7. These parameters are the lengths l_i (i=1 to 5) and the angle θ_{12}, defined keeping constant the maximum sphere (object) diameter D_{MAX} and the rover width H. Only a symmetric grasp will be considered in this phase.

The mechanism geometry was defined by a step by step procedure. In any case, the contact points between gripper and grasped object are always three, never located on a same object hemisphere, this to have a stable grasp, like it occurs for a human hand grasping an object with three contact points: thumb, another finger and palm.

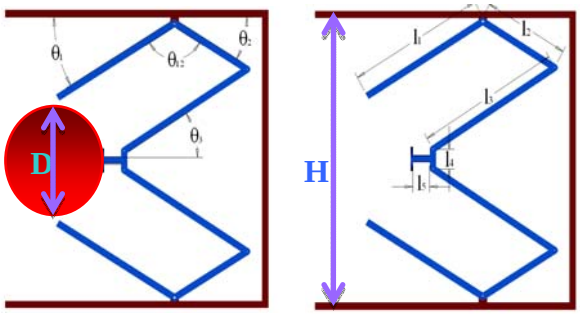

Figure 7 Gripper scheme and geometric parameters.

The geometric model is given in Eq. (1) to (5).

$$\theta_1 = arcsin\left(\frac{H-D}{2\cdot l_1}\right) \quad (1)$$

$$\theta_2 = \pi - (\theta_1 + \theta_{12}) \quad (2)$$

$$l_{3x} = l_1\cdot\cos(\theta_1) + l_2\cdot\cos(\theta_2) - \left(\frac{D}{2} + l_5\right) \quad (3)$$

$$l_{3y} = \frac{H}{2} - \left(\frac{l_4}{2} + l_2\cdot\sin(\theta_2)\right) \quad (4)$$

$$l_3 = \sqrt{(l_{3x})^2 + (l_{3y})^2} \quad (5)$$

The parameter l_3 will be computed knowing l_1, l_2, l_4, l_5, and θ_{12}. To know these last input parameters some encumbrance, kinetic and energy saving considerations are necessaries. In fact, the

parameters, respecting encumbrances and feature will be chosen to minimize the rover advance Δx, during the closing phase of grasping. The energy saving in the grasping phase, takes advantage from minimization of the rover advance Δx. In addition, this minimization avoids a too big centre of gravity position variation, of the loaded rover, during the grasping. Referring to the Fig. 8 will be done some encumbrance and feature considerations to define the parameters values.

The minimum l_1 value, acceptable to perform the all dimensions object grasping, is defined referring to the smaller sphere (object) grasped. In any case the maximum l_1 value must be such as to have the gripper within the frame overall dimensions. On the basis of that, for the overall rover dimension given above, the minimum and maximum values of l_1 are 0,45m and 0,80m respectively. The l_1 value will be chosen when the other parameters will be discussed.

For a given l_1, the length l_2 will be defined to minimize the rover advance Δx, during the closing phase of grasping, respecting a maximum value for l_2, lower the distance between the hinge (1) and the frame crosspiece (2) in Fig. 5.

This value of l_2 must respect a limit represented by an l_3 value, compatible with the foreseen object dimensions D and with the rover width, in Eq. (3) and (4).

About the l_4 and l_5 values, they will be between 0,05 and 0,2m because of the bumper assembling encumbrances. The chosen values will be 0,15m and 0,06m for l_4 and l_5 respectively.

For the angle θ_{12} the value is between a minimum of 90°, to allow the mechanism feature, and a maximum of 140°, to avoid interference with the rover frame of the l_2 arm.

For the angle θ_3, the value must be lower than 90°, to allow the mechanism movement (see Fig. 7). In any case it is convenient to have an angle θ_3 as little as possible, to have a bigger θ_2 excursion for a given Δx advance.

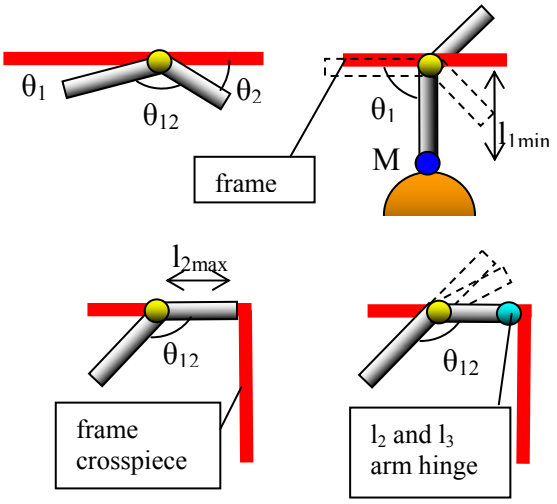

Figure 8 Encumbrance conditions graphs to choose the gripper geometrical parameters.

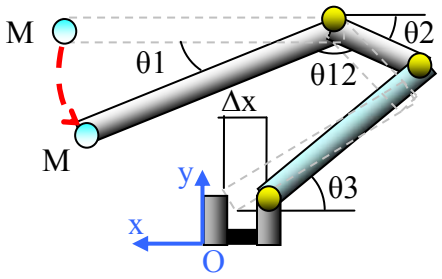

Figure 9 A detail of the gripper with Δx and θ_1 ratio.

To minimise the rover advance Δx it is convenient a low θ_1, this implies an high l_1. as expressed by the following Eq. (6), from Fig. 9.

$$\Delta x = l_2 \cdot \sin\left(\Delta\theta_1 + \left(\theta_{12} - \pi/2\right)\right) - l_2 \cdot \sin\left(\theta_{12} - \pi/2\right) \qquad (6)$$

On the contrary, this length value cannot be so high because of encumbrance and bending overload limits. On the basis of that the length of l_1 is fixed of 0.68m, θ_1 is then 26° for the bigger object. Having the l_1 value, it is possible to draw the point M trajectories, for different l_2 length that will be chosen for an efficient grab also of the minimum object, but minimizing Δx, as in Fig. 10, by Eq. (7) to (10). An efficient grasp is performed for l_2 lower than 0,2m for all object dimensions. Will be chosen a value for l_2 equal to 0,2m and not lower corresponding to a better grasp but to a too higher θ_3.

$$l_{2y} = l_2 \cdot \sin(\theta_2) \qquad (7)$$

$$\theta_3 = \arcsin\left(\frac{\frac{H}{2} - \left(\frac{l_4}{2} + l_{2y}\right)}{l_3}\right) \qquad (8)$$

$$x_m = l_1 \cos(\theta_1) + l_2 \cos(\theta_2) - (l_5 + l_3 \cdot \cos(\theta_3)) \qquad (9)$$

$$y_m = \frac{H}{2} - l_1 \sin(\theta_1) \qquad (10)$$

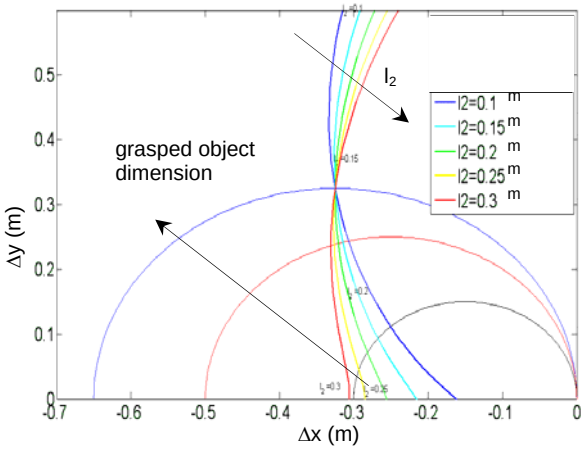

Figure 10 Point M trajectories, for different object dimensions and l_2 lengths.

The M position (Fig. 10) is given in a Cartesian frame of reference linked to the bumper as in Fig. 9.
The advance Δx is referred in Fig. 11 vs. the l_2 length for a given l_1; if l_1 is fixed also θ_1 is given, as shown in Fig. 9 for a given sphere (object) dimension. For a given l_2, for higher θ_{12}, Δx is lower. In any case θ_{12} must be lower then 140°, to avoid that the arm 2 exits from the rover frame overall dimensions.

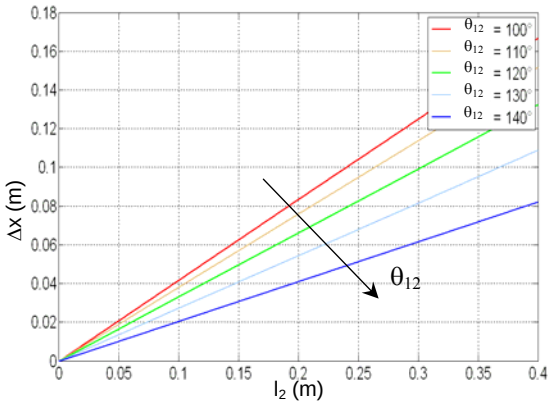

Figure 11 Δx trend vs. l_2 values, for given l_1 and fixed object dimension

The final chosen parameters values are:

l_1 = 0,68m
l_2 = 0,20m
l_4 = 0,15m
l_5 = 0,06m
θ_{12} = 120°

The computed values are:

l_5 = 0,57m
θ_{12} = 38°

5 MODELLING AND SIMULATION

Numerical simulations of the grasping system have been performed in MSC.ADAMS environment, for dynamic simulations due to its convenient features in simulating the operation of multi-body systems. To solve the differential equations of the dynamic model over a given interval of time was used the Gear Stiff Integrator (GSTIFF) that is the default in MSC.ADAMS environment; it takes advantage from a backwards differentiation formula to integrate differential and algebraic equation systems, assuming fixed time step (MSC.ADAMS, 2010).
To define the multi body model, the first step has been the definition of a suitable 3D CAD model of the gripper. This model has been imported into MSC.ADAMS environment and is completed with the needed joints, friction, contact forces and control functions to give the model shown in Fig. 8.

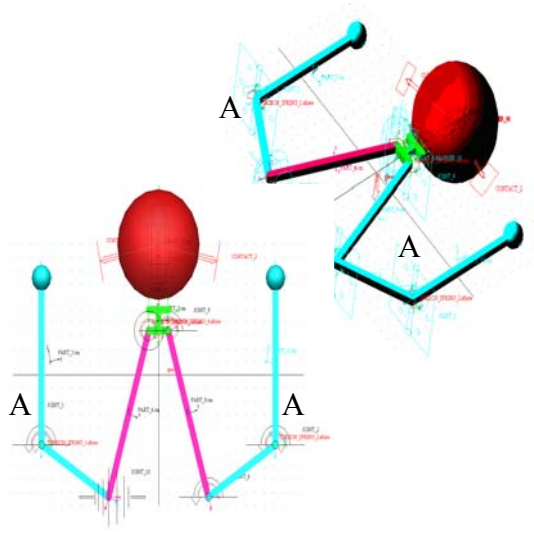

Figure 12 The multi body numerical model.

Referring to Fig. 12 the gripper is linked to the rover frame by two hinges A; the frame advances, driven by the motorized wheels.
The approaching, closing and grasping phases are shown in Fig. 13. The rover is driven by the motors moving the twin wheels on each of the four legs. This is represented in the multi body model by a driving force approaching the gripper towards the object. The friction coefficient, between different grippers arms in hinges, has been assumed with low values, as in usual robotic devices.
The driving force trend vs. time is represented in the graph (a) in Fig. 14. In the same figure are also referred the graphs showing the rover position (b) and the rover velocity (c) vs. time.
The driving force trend (a) is given equal to 1000N during approaching phase, reduced to 500N in the phase when the gripper is closed around the object. It can be seen that the rover position trend vs. time, represented in curve (b) allows to appreciate the gripper closing phase around the object. This phase can be divided in three steps. The first step corresponds to the rover advancing without contact respect to the object; the second one is when only the bumper is in contact with the object and the gripper is closing around the object; the third corresponds to the full three point contact between gripper and object, during the grasping. These three phases are schematically shown in Fig. 14.

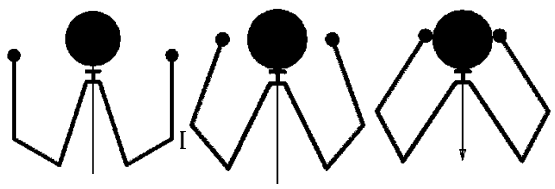

Figure 13 A grasping sequence.

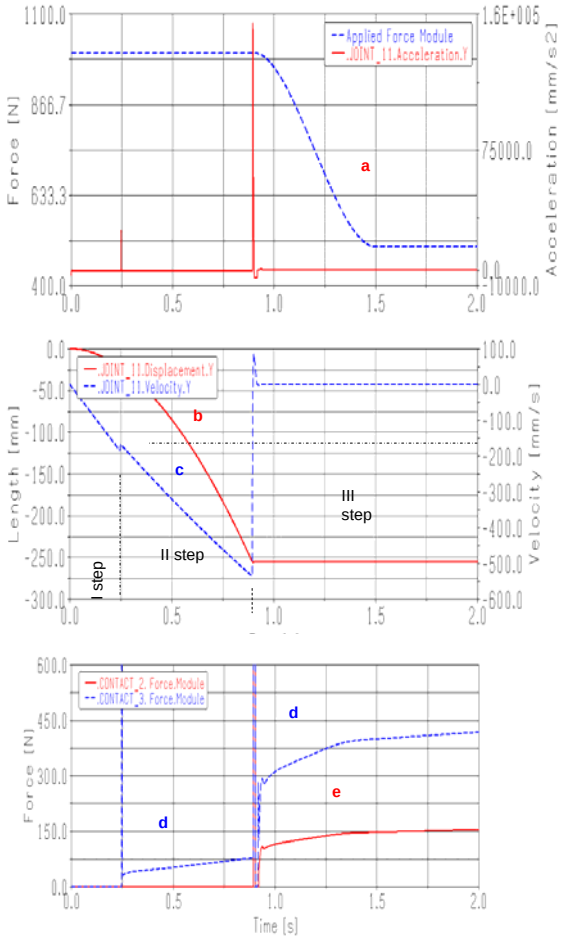

Figure 14 The driving force, rover position and velocity and the forces between gripper and object vs. time, in the multi body numerical model.

In the first step there is a constant acceleration of 0,7m/s^2, this step is about 0,25s long in time, the rover travels about 0,025m and the reached maximum velocity is 0,175m/s.

At the end of the first step there is the contact shock between the object and the bumper, this shock is highlighted in the velocity graph by a velocity sudden variation, this happens at a time of 0,25s from the start; the second step is 0,58s long in time, reaching, at the end, a time of 0,83 s from the start; the reached position from the start at the end of second step is 0,25m and the mean acceleration is lower then that in the previous step: the mean acceleration is about 0,34m/s^2.

At the end of the second step the velocity is about 0.525m/s; in the third step the rover stops when the object is completely gasped. In this last step it can be seen that the locking phase is 0,2s long. During this third step the rover driving force, referred in the graph in Fig. 14, is gradually reduced from 1000N to 500N.

In the graphs in Fig. 14 are referred also the resultant force between the object and the bumper and between the object and the gripper lateral palms in curves (d) and (e) respectively.

In the graph (d), referring the resultant force trend between the object and the bumper, at a time of 0,25s form the start, the curve shows a peak, this is due to inertial effects, because of the contact shock between bumper and object, after the force reaches again a value able to move the gripper closing around the object up to the contact between palms and object when the force trend, referred in curve (d), reaches a sudden high value due to the shock at the contact between palms and object. This appears at a time of 0,90s from the start. The rover is now stopped and the object grasped with a constant force on each palm of about 320N, in this situation a force of 800N acts on the bumper, as shown in curve (e).

6 CONCLUSION

This paper proposed an optimisation strategy to define the geometrical configuration of a gripper, among three preliminary configurations, for a lunar working rover. The gripper is designed avoiding a dedicated actuation to optimise reliability and to minimise weights. Among the three proposed scheme, one is chosen by overall considerations. An optimisation strategy was discussed and performed to define the gripper dimensions. The strategy is general and based on fundamental principles of gripper design. The multi body simulation developed within MSC.ADAMS environment indicates the gripper behaviour both in the approaching operation and in the grasping one, in different phases.

The optimisation and simulation processes are both used for a given purpose, but they may be useful in different gripper or robotic design approaches.

ACKNOWLEDGEMENTS

Partial support of this research by the Italian Ministry of Research is gratefully acknowledged.

REFERENCES

[1] Ambu, R., Manuello Bertetto, A., Falchi, C. 2010. A Working Lunar Rover: Passive Gripper Mechanism and Actuated Leg. In: Proceedings of the *19th International Workshop On Robotics In Alpe-Adria-Danube Region*. Budapest - Hungary, 23-27 June.

[2] Benaroya, H., Bernold, L., and Meng Chua, K. 2002 Engineering, Design and Construction of Lunar Bases, *Journal of Aerospace Engineering*, pp. 33-45.

[3] Benaroya, H., Bernold, L. 2008. Engineering of Lunar Bases, *Acta Astronautica*, Vol. 62, pp. 277–299.

[4] Ceccarelli, M., 2004. Fundamentals of Mechanics of Robotic Manipulation, *Kluwer Academic Publisher.*

[5] Dechev, N, Cleghorn, WL, Nauman, S. 1999 Multiple finger, passive adaptive grasp prosthetic hand. *Mechanism and Machine Theory* Vol. 36, pp. 1157–1173.

[6] Iberal, T., 1997. Human prehension and dexterous robot hands. *International Journal of Robotics Research*; Vol 6(3), pp. 285–299.

[7] Johnson, S.W and Wetzel, J.P. 1988. Engineering, construction and operations in space, *New York, ASCE*.

[8] Manuello Bertetto, A., Ruggiu, M. 2003. A two degree of freedom gripper actuated by SMA with flexure hinges. *JOURNAL OF ROBOTIC SYSTEMS*, Vol. 20, pp. 649-657, ISSN: 0741-2223

[9] Pham, DT, Heginbotham, WB. 1986. Robot grippers. Bedford: *IFS Publications Ltd.*;. NEW YORK: IEEE - USA, ISBN/ISSN: 978-1-4244-6884-3.

[10] Venkataraman, ST, Iberall, T. 1989. Dexterous robot Hands. *New York: Springer-Verlag*.

[11] MSC.ADAMS, 2010. Documentation and Help, User CD-ROM.

ISSN 1590-8844
International Journal of Mechanics and Control, Vol. 14, No. 01, 2013

TEMPLATE FOR PREPARING PAPERS FOR PUBLISHING IN INTERNATIONAL JOURNAL OF MECHANICS AND CONTROL

Author1* Author2**

* affiliation Author1

** affiliation Author2

ABSTRACT

This is a brief guide to prepare papers in a better style for publishing in International Journal of Mechanics and Control (JoMaC). It gives details of the preferred style in a template format to ease paper presentation. The abstract must be able to indicate the principal authors' contribution to the argument containing the chosen method and the obtained results. (max 200 words)

Keywords: keywords list (max 5 words)

1 TITLE OF SECTION (E.G. INTRODUCTION)

This sample article is to show you how to prepare papers in a standard style for publishing in International Journal of Mechanics and Control.
It offers you a template for paper layout, and describes points you should notice before you submit your papers.

2 PREPARATION OF PAPERS

2.1 SUBMISSION OF PAPERS

The papers should be submitted in the form of an electronic document, either in Microsoft Word format (Word'97 version or earlier).
In addition to the electronic version a hardcopy of the complete paper including diagrams with annotations must be supplied. The final format of the papers will be A4 page size with a two column layout. The text will be Times New Roman font size 10.

Contact author: author1[1], author2[2]

[1]Address of author1.
[2]Address of author2 if different from author1's address
E-mail: author1@univ1.com , author2@univ2.com

2.2 DETAILS OF PAPER LAYOUT

2.2.1 Style of Writing

The language is English and with UK/European spelling. The papers should be written in the third person. Related work conducted elsewhere may be criticised but not the individuals conducting the work. The paper should be comprehensible both to specialists in the appropriate field and to those with a general understanding of the subject.
Company names or advertising, direct or indirect, is not permitted and product names will only be included at the discretion of the editor. Abbreviations should be spelt out in full the first time they appear and their abbreviated form included in brackets immediately after. Words used in a special context should appear in inverted single quotation mark the first time they appear. Papers are accepted also on the basis that they may be edited for style and language.

2.2.2 Paper length

Paper length is free, but should normally not exceed 10000 words and twenty illustrations.

2.2.3 Diagrams and figures

Figures and Tables will either be entered in one column or two columns and should be 80 mm or 160 mm wide respectively. A minimum line width of 1 point is required at actual size. Captions and annotations should be in 10 point with the first letter only capitalised *at actual size* (see Figure 1 and Table VII).

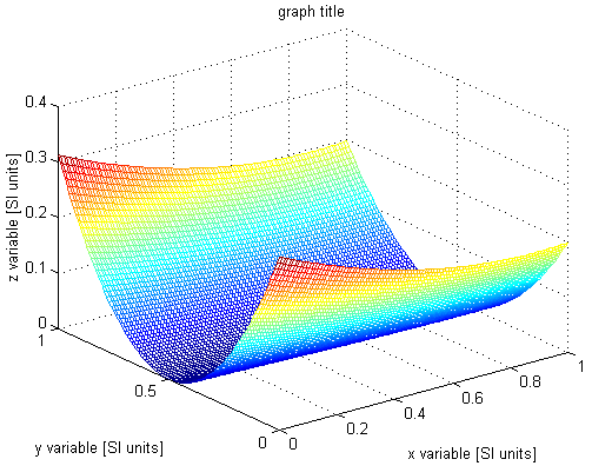

Figure 1 Simple chart.

Table VII - Experimental values

Robot Arm Velocity (rad/s)	Motor Torque (Nm)
0.123	10.123
1.456	20.234
2.789	30.345
3.012	40.456

2.2.4 Photographs and illustrations

Authors could wish to publish in full colour photographs and illustrations. Photographs and illustrations should be included in the electronic document and a copy of their original sent. Illustrations in full colour …

2.2.5 Equations

Each equation should occur on a new line with uniform spacing from adjacent text as indicated in this template. The equations, where they are referred to in the text, should be numbered sequentially and their identifier enclosed in parenthesis, right justified. The symbols, where referred to in the text, should be italicised.

- point 1
  - point 2
    - point 3

1. numbered point 1
   2. numbered point 2
      3. numbered point 3

$$W(d) = G(A_0, \sigma, d) = \frac{1}{T}\int_0^{+\infty} A_0 \cdot e^{-\frac{d^2}{2\sigma^2}} dt \qquad (1)$$

3 COPYRIGHT

Authors will be asked to sign a copyright transfer form prior to JoMaC publishing of their paper. Reproduction of any part of the publication is not allowed elsewhere without permission from JoMaC whose prior publication must be cited. The understanding is that they have been neither previously published nor submitted concurrently to any other publisher.

4 PEER REVIEW

Papers for publication in JoMaC will first undergo review by anonymous, impartial specialists in the appropriate field. Based on the comments of the referees the Editor will decide on acceptance, revision or rejection. The authors will be provided with copies of the reviewers' remarks to aid in revision and improvement where appropriate.

5 REFERENCES (DESCRIPTION)

The papers in the reference list must be cited in the text. In the text the citation should appear in square brackets [ ], as in, for example, "the red fox has been shown to jump the black cat [3] but not when...". In the Reference list the font should be Times New Roman with 10 point size. Author's first names should be terminated by a 'full stop'. The reference number should be enclosed in brackets.

The book titles should be in *italics*, followed by a 'full stop'. Proceedings or journal titles should be in *italics.* For instance:

REFERENCES (EXAMPLE)

[1] Smith J., Jones A.B. and Brown J., *The title of the book*. 1st edition, Publisher, 2001.

[2] Smith J., Jones A.B. and Brown J., The title of the paper. *Proc. of* C*onference Name*, where it took place, Vol. 1, paper number, pp. 1-11, 2001.

[3] Smith J., Jones A.B. and Brown J., The title of the paper. *Journal Name*, Vol. 1, No. 1, pp. 1-11, 2001.

[4] Smith J., Jones A.B. and Brown J., *Patent title*, U.S. Patent number, 2001.

International Journal of Mechanics and Control – JoMaC
Published by Levrotto&Bella
TRANSFER OF COPYRIGHT AGREEMENT

NOTE: Authors/copyright holders are asked to complete this form signing section A, B or C and mail it to the editor office with the manuscript or as soon afterwards as possible.	*Editor's office address:* Andrea Manuello Bertetto Elvio Bonisoli *Dept. of Mechanics* *Technical University – Politecnico di Torino* *C.so Duca degli Abruzzi, 24 – 10129 Torino – Italy* *e_mail: jomac@polito.it* *fax n.: +39.011.564.6999*

The article title:

By:_____

To be Published in ***International Journal of Mechanics and Control JoMaC***
Official legal Turin court registration Number 5320 (5 May 2000) - reg. Tribunale di Torino N. 5390 del 5 maggio 2000

A Copyright to the above article is hereby transferred to the JoMaC, effective upon acceptance for publication. However the following rights are reserved by the author(s)/copyright holder(s):
1. All proprietary rights other than copyright, such as patent rights;
2. The right to use, free or charge, all or part of this article in future works of their own, such as books and lectures;
3. The right to reproduce the article for their own purposes provided the copies are not offered for sale.

To be signed below by all authors or, if signed by only one author on behalf of all co-authors, the statement A2 below must be signed.

A1. All authors:

SIGNATURE_____DATE_____ SIGNATURE_____DATE_____

PRINTED NAME_____ PRINTED NAME_____

SIGNATURE_____DATE_____ SIGNATURE_____DATE_____

PRINTED NAME_____ PRINTED NAME_____

A2. One author on behalf of all co-authors:
"I represent and warrant that I am authorised to execute this transfer of copyright on behalf of all the authors of the article referred to above"

PRINTED NAME_____

SIGNATURE_____ TITLE_____ DATE_____

B. The above article was written as part of duties as an employee or otherwise as a work made for hire. As an authorised representative of the employer or other proprietor. I hereby transfer copyright to the above article to *International Journal of Mechanics and Control* effective upon publication. However, the following rights are reserved:
1. All proprietary rights other than copyright, such as patent rights;
2. The right to use, free or charge, all or part of this article in future works of their own, such as books and lectures;
3. The right to reproduce the article for their own purposes provided the copies are not offered for sale.

PRINTED NAME_____

SIGNATURE_____ TITLE_____ DATE_____

C. I certify that the above article has been written in the course of employment by the United States Government so that no copyright exists, or by the United Kingdom Government (Crown Copyright), thus there is no transfer of copyright.

PRINTED NAME_____

SIGNATURE_____ TITLE_____ DATE_____

CONTENTS

next number scheduled titles:

Epi.q-1.2, A Hybrid Mobile Mini Robot with a Reconfigurable Three Wheeled Locomotion Unit
G. Quaglia, W. Franco, D. Maffiodo, S. Appendino and R. Oderio

Optimization of Thermal Control and Energy Saving for Space Multifunctional Structures
Eleonora Zeminiani, Michele Cencetti and Paolo Maggiore

Nonlinear Energy Harvester for Wireless Mouse Device
E. Bonisoli, F. Di Monaco, N. Manca

Proposal of Innovative Fluid Dynamic Nonlinear Servovalve Synthethic Models
P. Alimhillaj, L. Borello and M. D. L. Dalla Vedova

The Mechanism of Crank Initiation and Propagation in Metallic Engineering Materials
V.T. Hoang